FPL.

L-2013-094
10 CFR 52.3

March 21, 2013

U.S. Nuclear Regulatory Commission
Attn: Document Control Desk
Washington, D.C. 20555-0001

Re: Florida Power & Light Company
Proposed Turkey Point Units 6 and 7
Docket Nos. 52-040 and 52-041
Revised Response to NRC Request for Additional Information
Letter No. 047 (eRAI 6225) Standard Review Plan Section
02.04.06 Probable Maximum Tsunami Flooding

Reference:

1. NRC Letter to FPL dated December 21, 2011, Request for Additional Information Letter No. 047 Related to SRP Section 02.04.06 Probable Maximum Tsunami Flooding for the Turkey Point Nuclear Plant Units 6 and 7 Combined License Application
2. FPL Letter L-2012-295 to NRC dated July 26, 2012, Response to NRC Request for Additional Information Letter No. 047 (eRAI 6225) Standard Review Plan Section 02.04.06 Probable Maximum Tsunami Flooding
3. Notice of Forthcoming Public Meeting to Discuss Response to Final Assessment of the Probable Maximum Tsunami Issues Related to Turkey Point Units 6 & 7 Combined License Application, dated October 31, 2012 (ML12300A325).
4. Mulder T., E. Ducassou , G.P. Eberli, V. Hanquiez , E. Gonthier , P. Kindler, M. Principaud , F. Fournier, P. Léonide, I. Billeaud, B. Marsset, J.J.G. Reijmer, C. Bondu, R. Joussiaume, and M. Pakiades, “New insights into the morphology and sedimentary processes along the western slope of Great Bahama Bank”, Geology, July 2012; vol. 40; no. 7; pp. 603–606, 2012.

Florida Power & Light Company (FPL) provided its revised response to the Nuclear Regulatory Commission’s (NRC) Request for Additional Information (RAI) 02.04.06-7 (Reference 1) in FPL letter L-2012-295 dated July 26, 2012 (Reference 2.)

The response is being revised as a result of comments received during the public meeting held between the NRC and FPL on November 15, 2012 (Reference 3). In this revision to Reference 2, FPL has provided additional information to respond to the original Request for Additional Information (RAI) 02.04.06-7. The additional information

D097
NRO

discusses the impact of potential tsunamis generated by submarine slope failures along the western margin of the Great Bahama Bank (GBB). The revised response also considered recent information by Mulder et al. (Reference 4). The additional information does not impact any conclusions in Subsection 2.4.6 of the Final Safety Analysis Report.

The attachment identifies any changes that will be made in a future revision of the Turkey Point Units 6 and 7 Combined License Application (if applicable).

If you have any questions, or need additional information, please contact me at 561-691-7490.

I declare under penalty of perjury that the foregoing is true and correct.

Executed on March 21, 2013

Sincerely,

William Maher
Senior Licensing Director – New Nuclear Projects

WDM/RFB

Attachment: FPL Revised Response to NRC RAI No. 02.04.06-7 (eRAI 6225)

cc:
PTN 6 & 7 Project Manager, AP1000 Projects Branch 1, USNRC DNRL/NRO
Regional Administrator, Region II, USNRC
Senior Resident Inspector, USNRC, Turkey Point Plant 3 & 4

NRC RAI Letter No. PTN-RAI-LTR-047

SRP Section: 02.04.06 – Probable Maximum Tsunami Flooding

Question from Hydrological and Meteorology Branch (RHMB)

NRC RAI Number: 02.04.06-7 (eRAI 6225)

To meet the requirements of GDC 2, 10 CFR 52.17, and 10 CFR Part 100, FPL should provide an assessment of the Probable Maximum Tsunami (PMT) for the proposed site. Section C.I.2.4.6.3 of Regulatory Guide 1.206 (RG 1.206) provides specific guidance with respect to the source characteristics needed to determine the PMT. Provide justification that triggering conditions for submarine mass failures in the Florida Straits are not currently present. If triggering and pre-conditioning factors/loading conditions such as those that caused the Miocene debris flows and likely Pleistocene-age failures at the western end of the Florida Straits (Holmes, 1985; Twichell and others, 1993) cannot be determined, explain whether potential submarine mass failures can be conservatively excluded. If such failures are considered, discuss how inclusion of this source affects PMT water levels at the site.

References

Holmes, C.W., 1985, Accretion of the South Florida Platform, Late Quaternary development: American Association of Petroleum Geologists Bulletin, v. 69, p. 149-160.

Twichell, D.C., Valentine, P.C., and Parson, L.M., 1993, Slope failure of carbonate sediment on the West Florida Slope, *in* Schwab, W.C., Lee, H.J., and Twichell, D.C., eds., Submarine Landslides: Selected Studies in the U.S. Exclusive Economic Zone: U.S. Geological Survey Bulletin 2002, p. 69-78.

FPL RESPONSE:

As a result of comments received during the public meeting held between the NRC and FPL on November 15, 2012 (Reference 20), FPL has provided additional information to respond to the original Request for Additional Information (RAI) Item 02.04.06-7. The additional information discusses the impact of potential tsunamis generated by submarine slope failures along the western margin of the Great Bahama Bank (GBB).

Part A of this response provides information focused on the tsunami events from potential slides in the Florida Escarpment. This information was provided to the NRC in Reference 19 and has not been revised. The title *Part A – Evaluation of Tsunamis Generated from Submarine Slides in the Florida Escarpment* has been added to the previous response.

Part B of this response documents the work performed to assess the impact of a potential tsunami generated by submarine slope failures along the western margin of the GBB. The slope failure location and dimensions are postulated based on published information and provide conservative input to model a quantitative estimate of the flood level at the Turkey Point Units 6 & 7 site. The results indicate that the maximum water level at the Turkey Point Units 6 & 7 site caused by a tsunami from a GBB submarine landslide would be lower than the maximum water level for the probable maximum tsunami (PMT) case reported in FSAR Subsection 2.4.6.5.

Part A – Evaluation of Tsunamis Generated from Submarine Slides in the Florida Escarpment

Submarine landslide zones in the Gulf of Mexico including the Florida Escarpment have been evaluated in FSAR 2.4.6.1.2. Based on information from published literature and physical reasoning, it was concluded that tsunamis generated from these landslide sources would not affect the safety related facilities at the Turkey Point Units 6 & 7 site. In response to RAI 02.04.06-7 and follow-on clarifications from NRC, FPL elects to supplement the FSAR evaluation with numerical model simulations, using the NHWAVE and FUNWAVE codes developed and maintained by University of Delaware, to provide a quantitative estimate of the flood level at the site and reaffirm that the tsunami source of concern will not affect the probable maximum tsunami (PMT) flood level reported in the FSAR.

This response provides additional information from the review of the published literature and data on the potential slides on the southern part of the Florida Escarpment near the western end of the Florida Straits. It is followed by the characterization of the postulated tsunami source and a detailed description of the numerical modeling approach used to simulate the initial surface deformation generated by such a failure, the propagation of the tsunami wave towards the site and the resulting coastal inundation.

The response concludes with a summary of the key results from the model simulations, which show that the maximum water level at the site of Turkey Point Units 6 and 7 caused by a tsunami from the Florida Escarpment slide would be lower than the maximum water level for the PMT case reported in FSAR Section 2.4.6.5.

The West Florida Escarpment Slide

The West Florida Escarpment is the major marine geomorphic feature on the west coast of Florida (Figure 1). It has undergone significant erosion since its initial formation during the Cretaceous as part of a reef complex with as much as 8 kilometers of erosional retreat of its base (Reference 1). In general, the slope on the West Florida Escarpment increases below 1750 meters depth and frequently exceeds 40 degrees. The front of the escarpment is composed of Lower and Middle Cretaceous platform-interior bedded lagoonal limestones and dolostones. Accumulations of younger Pliocene and Pleistocene sediments associated with the Mississippi Fan (submarine deltaic deposits from the Mississippi Embayment) onlaps at the base of the escarpment (References 1 and 2).

A study was conducted in 1985 using SeaBeam bathymetric data and GLORIA (Geologic LOng-Range Inclined Asdic) side-scan sonar data collected by the USGS and the Institute of Oceanographic Sciences of the United Kingdom to examine the submarine mass failures in the West Florida Escarpment. The GLORIA images covered a broad area of about 220-kilometers in length along the escarpment between 25° N and 27° N. This study concluded that erosion has occurred since the initial formation of the escarpment and that erosional processes changed its morphology at different rates (Reference 5).

In the area north of 27° N the escarpment is a relatively linear landform with slope gradients of less than 28 degrees and is dissected by numerous valleys spaced 1 to 5 kilometers apart with tributary gullies feeding into them (Reference 1 Figure 6-2). The Cenozoic sediments in this area have not been exposed to extensive erosion due to the presence of the thin discontinuous Cenozoic sediment cover as well as possible undisturbed reef structures in the underlying Cretaceous section. The slope above this part of the escarpment is smooth and is interrupted by only a few mass wasting scarps. Below the escarpment are aprons (as seen in GLORIA imagery and SeaBeam bathymetry, (Reference 1, Figure 6-2)) which are inferred to be carbonate debris material that have been eroded and transported off the escarpment and interfinger with late Pleistocene-age fan deposits (Reference 1).

South of 27° N part of the escarpment is also relatively linear but is terraced and parts are deeply incised by large canyons. On the straight part of the escarpment, which occurs between 25.5° N and 26.5° N, the lower part of the escarpment is terraced whereas the upper part is steeper and unterraced (Reference 1, Figure 6-3). The terraces have gradients of 10 to 20 degrees while the terrace risers and the upper part of the escarpment have gradients of 30 to 42 degrees. The canyons incised the edge of the Florida platform by as much as 15 kilometers. The canyon heads are 1 to 3 kilometers wide and the mouths are 3 to 7 kilometers wide (Reference 1, Figure 6-4). The canyon's floors are flat and at the same depth as the abyssal plain floor except immediately below. The canyon's headwalls where the depressions occur are as much as 80 meters deeper than the abyssal plain floor. Talus deposits that have been eroded from the headwalls are seen in the GLORIA image (Reference 1, Figure 6-4).The headwalls have gradients that exceed 40 degrees and do not have terraces; however, the sidewalls are not as steep and do have discontinuous terraces. These canyons are called box canyons and are concentrated in two groups along the southern part of the escarpment. One group occurs between 26.5° N and 27° N and the second between 24.3° N and 25.6° N (Reference 1).

The area that is postulated to be the site of a maximum credible submarine landslide is identified along the southern part of the West Florida Slope as delineated in Figure 2 (Reference 7). Doyle and Holmes (Reference 4) and Twichell et al. (Reference 5) have stated that this area has undergone collapse. The area is described as characterized by "scarps (that) are still exposed on the seafloor and have 50-150 meters relief and are 10-70 kilometers in length" (Reference 7). According to ten Brink et al. (Reference 7), "some of the mass movement deposits are on the slope above the Florida Escarpment, but it is unknown how much of the failed material was transported farther and deposited at the base of the Florida Escarpment." These landslides from the West Florida Slope are composed of several smaller failure events as seen in the cross cutting relationships of the headwall scarps in the imagery (Reference 5). The age of these failures is not known, but it is suggested by Mullins et al. (Reference 3) and Doyle and Holmes (Reference 4) that periods of increased mass wasting are associated with periods of higher sedimentation rates. Therefore, it is possible that the landslides along the southern part of the West Florida Slope are likely early Holocene (4500-10,000 years before the present) or older in age (Reference 6). The runout distance of the existing slope failure is uncertain, as landslide deposits at the base of the West Florida Escarpment are buried under younger Mississippi Fan Deposits (Reference 7).

Representation of the Florida Escarpment Slide in the Model Simulations

The maximum credible slide at the Florida Escarpment that is a potential tsunami source was schematized for modeling purposes as having a Gaussian shape with an elliptical footing. This shape was chosen because a Gaussian shape has been used for several investigations and studies of landslide tsunamis, including benchmark cases (References 9, 14, 18). Grilli and Watts (Reference 9) state that a Gaussian shape is a more realistic representation of a submarine mass failure than other arbitrary fixed shapes. Enet & Grilli (Reference 8) used a Gaussian shape in the experiments that provide the basis for the validation of the model used to simulate the generation of a wave by a submarine slide (Reference 8). The Gaussian shape of the slide was approximated in the numerical model by truncated hyperbolic secant squared functions (Reference 8). The elliptical base of the slide was located in a manner that covers as closely as possible the maximum credible submarine slide above the Florida Escarpment as delineated in Reference 7 and shown in Figure 3. Based on this placement of the base of the slide prior to the initiation of movement its centroid is located at 25.92° N, 84.80° W (Figure 3). The length (minor axis of the elliptical base) of the slide shown in Figure 3 is 19.2 kilometers, and the width (major axis of its elliptical base) of the slide is approximately 42.9 kilometers. These dimensions were selected so the ellipse approximately covers the area of the outline of maximum credible submarine slide above the Florida Escarpment, and it has an area equal to 647.57 square kilometers (Reference 7).

The maximum thickness of the slide was postulated to be approximately 66 meters, calculated based on a volume of 16.2 cubic kilometers as estimated from bathymetric data (Reference 7) of the schematized slide used in the model.

The bottom slope used in the model was 5.8 degrees. This slope was estimated based on the water depth difference between the centroid of the slide at its initial position and a point downslope at a distance equal to the minor axis of the elliptical base of the slide, i.e., 19.2 kilometers. The water depth at these two points is 1355 and 3307 meters, respectively, as obtained from the bathymetric data used for the model (Reference 16). The depths of these two points are shown also in Figure 7(b).

The initial acceleration of the slide, 0.992 meters per second squared, is estimated directly from the bed slope. The terminal velocity of the slide was estimated as equal to 134.3 meters per second. This estimate was obtained using a specific gravity for the slide equal to 2, and a bed slope of 5.8 degrees and a length of 19.2 kilometers. The global drag coefficient was assumed to be equal to 1 (Reference 9), which is conservative. Based on its initial acceleration the slide reaches its terminal velocity within 135 seconds.

Initial Wave Generated by the Florida Escarpment Slide

Two alternative approaches were used for the generation of the initial wave in the tsunami simulations. The two approaches are referred to as the dynamic source approach and the static source approach. Two source approaches are used as the velocity components from the dynamic source can differ significantly from the static source with respect to the total slide energy.

The dynamic source approach defined the initial condition for the tsunami propagation simulations in terms of both the water surface displacement and the depth-averaged horizontal velocity fields. This source was computed from the slide geometry and its movement using the computer model NHWAVE (Non-Hydrostatic Wave), Version 1.1 (Reference 10). NHWAVE solves the fully non-hydrostatic Navier-Stokes equations in the sigma coordinate system. The model assumes a single-valued water surface and represents turbulent stresses in terms of an eddy viscosity closure scheme. Turbulent stresses are not modeled in the Florida Escarpment simulations, and thus the model is basically solving the Euler equations for incompressible flow with a moving surface and bottom.

Input to NHWAVE includes the bathymetric grid, the slide dimensions, the initial slide position and orientation, and the terminal velocity. The modeled domain was set up so that the landslide event was centrally located and the generated motion did not reach the lateral boundaries during the simulated time. Bathymetric data for the model domain of NHWAVE and the three nested grids of FUNWAVE-TVD used in the simulations were obtained from the National Geophysical Data Center (NGDC) ETOPO 1 (Reference 16) and the Coastal Relief Model (CRM) (Reference 17) data sets.

The assumed runout distance of the slide volume as it moves downslope along its minor axis is 24.5 kilometers. It is the distance between the centroid of the elliptical base of the slide in its initial position and the intersection of an extension of the bottom slope at the initial position of the slide and the sea floor at the base of the escarpment. This is a very conservative assumption, because the sea floor beyond 9.6 kilometers from the initial position of the centroid of the slide is practically horizontal. Therefore, assuming that the slide will continue moving at the same velocity up to 24.5 kilometers from its initial position would produce conservative estimates of the initial wave. The present approach neglects the spreading and flattening of the sliding mass during the slide process in the present simulations. This results in a higher and narrower initial elevation hump at the final slide location than what would have occurred if the slide were allowed to deform. The initial and final positions of the slide are displayed in Figure 5.

The NHWAVE model was run for a period of time and the surface displacement field and horizontal velocity fields at 250 seconds, the time required to travel the postulated run out distance of 24.5 kilometers, were saved and used as input into FUNWAVE-TVD, Version 1.1 (Reference 15). The resulting water surface displacement from NHWAVE at that time (250 seconds) is shown in Figure 6 and Figure 7, which also shows the water surface profile in the direction of the slide motion simulated with NHWAVE at different times after the initiation of the slide. As shown in Figure 7 the maximum water surface at 250 seconds is 47.2 meters, and the minimum –77.5 meters.

The second approach to the generation of the initial condition for the tsunami propagation model used a static source based on the geometry of the initial and final positions of the slide mass. A static source is defined as an initial displacement of the water surface in the form of a depression over the initial slide location, equal in areal extent, shape and volume to the displaced material volume during the submarine slide. It was assumed that the initial slide volume described above translates downslope along its axis in the direction of the slope beyond its original footprint. A positive displacement of the water surface equal to the volume, shape and size of the slide was assumed at that point, i.e., extending over an elliptical area with minor axis equal to 19.2 kilometers, major axis 42.9 kilometers and maximum thickness 66 meters, and a corresponding negative displacement representing the missing volume of the slide mass was assumed over the initial position of the slide. The centroid of the depression of the water surface was placed at 25.92° N, 84.80° W, same as the initial location of the centroid of the slide for the dynamic source. A water rise equal in shape and size with the depression was assumed downslope of the initial depression and at a distance equal to translation distance of the dynamic case, i.e., 24.5 kilometers. The maximum water surface rise is equal to 66 meters. Figure 20 shows the assumed initial water surface wave for the Florida Escarpment tsunami simulation with FUNWAVE-TVD based on a static source. Using an initial static source, it was assumed that the initial horizontal velocities were zero over the entire model domain of FUNWAVE-TVD.

Modeling of Tsunami Propagation and Inundation

The propagation, shoreline runup and inundation caused by the Florida Escarpment tsunami were simulated using the Boussinesq wave model FUNWAVE-TVD, developed at the University of Delaware. In its present application, FUNWAVE-TVD solved the spherical-polar form of the weakly-nonlinear, weakly-dispersive Boussinesq equations described in Reference 11. Reference 12 describes the operation of both Cartesian and spherical-polar versions of the code. The model incorporates bottom friction and subgrid lateral turbulent mixing effects.

The Cartesian coordinate version of FUNWAVE-TVD, described in References 12 and 13, has been validated using several PMEL-135 benchmarks (Reference 14), which are the presently accepted benchmarking standards adopted by the National Tsunami Hazard Mitigation Program (NTHMP) for judging model acceptance for use in development of coastal inundation maps and evacuation plans. Benchmark tests for the Cartesian version of FUNWAVE-TVD are described in Reference 12. Benchmark tests for the spherical version of the code are described in Reference 11.

The equations solved by FUNWAVE-TVD consist of a depth-integrated volume conservation equation together with depth-integrated horizontal momentum equations. These equations are summarized in References 12 and 13. For tsunami applications, FUNWAVE-TVD is run with closed boundaries and an initial hot start condition consisting of either a surface displacement alone (in the case of static initial conditions) or a surface displacement and initial velocity field (in the case of a dynamic initial condition based on the results of calculations with NHWAVE). The model is run from the initial start until past the time when significant wave activity has decayed at the target site.

In most large scale problems FUNWAVE-TVD is run on multiple nested grids. The grid nesting scheme uses a one-way nesting technique, which passes surface elevation and velocity components calculated from a large domain to a nested small domain through ghost cells at nesting boundaries. A linear interpolation is performed between the large and the small domain at the nesting boundaries. A test of the nesting process is included in the FUNWAVE-TVD verification and validation document (Reference 11).

In the simulations of the Florida Escarpment tsunami three nested grids are used, which are referred to as Grid A, Grid B, and Grid C. The output from Grid A is used as input to FUNWAVE-TVD on Grid B. The same process is repeated in going from Grid B to Grid C.

The domain covered by each of these three grids is shown in Figure 4. All the grids are based on geographic coordinates. The coordinates of the southwest corner of each grid, the grid spacing and number of grid cells in each grid of the three grids are given in Table 1.

Table 1. Nested grids used in FUNWAVE-TVD

Grid	Coordinates of SW Corner		Grid Spacing	Number of Grid Cells
	x	y	□x = □y	
	degrees	degrees	seconds	Cells
A	-89.0	22.0	60	780 x 420
B	-80.75	23.0	15	480 x 1260
C	-80.517	25.156	3	592 x 768

It is noted that because of the curvature of the earth, having a uniform grid size in degrees leads to variable-length (in the west-east direction) cells at different latitudes within the model domain.

There is a sponge layer along the open boundaries of the model which was used for the definition of the boundary conditions. The thickness of the sponge layer was 200 kilometers along the eastern and northern boundaries, 100 kilometers along the southern boundary and 150 kilometers along the western boundary.

The antecedent water surface level used for the model simulation was equal to the 10 percent exceedance high tide level, plus the initial rise and long term sea level rise, which produce an initial water level equal to 1.68 meters (5.5 feet) mean low water (MLW), or 3.6 feet (1.10 meters) NAVD 88, same as that used for the PMT numerical simulation in FSAR 2.4.6.4 and for the probable maximum storm surge evaluation as explained in FSAR 2.4.5.2.2.1.

Simulation Results

Two sets of simulation results for the tsunami propagation and inundation by the Florida Escarpment tsunami are presented. The first set of results is for the dynamic initial condition and the second set of results is for the static initial condition.

<u>Dynamic Source Initial Condition</u>

Figure 8 and Figure 9 show the propagation of the tsunami wave over the domain of model Grid A during the first three hours after the generation of the initial wave by the slide, presenting snapshots of the wave height every 20 minutes. Time zero in the FUNWAVE-TVD simulation is 250 seconds after the initiation of the slide. It should be noticed that the color scale indicating wave height differs in the different panels of these two figures. Figure 10 shows the maximum water surface elevation within the model domain of Grid A during the simulation period. The highest water levels are in the vicinity and to the west of the slide.

Figure 11 and Figure 12 show the propagation of the tsunami wave in Grid B, from 80 minutes in the FUNWAVE-TVD simulation, and after the wave enters the Grid B domain, until 240 minutes. Snapshots of the wave height every 20 minutes are shown. Figure 13 shows the maximum water surface elevation within the model domain of Grid B during the simulation period. The maximum water level rise within the domain of Grid B is less than 0.1

m. As shown in Figure 13, the highest water levels occur over a relatively shallower area between Florida and Cuba, which can be seen in Figure 4.

Figure 14 and Figure 15 show the propagation of the tsunami wave in Grid C, from 140 minutes until 240 minutes in the simulation. Snapshots of the wave height every 20 minutes are shown. Figure 16 shows the maximum water level over Grid C. As can be seen in these figures, the area surrounding the site of Units 6 & 7 is inundated. However, the Units 6 & 7 site itself and other parts of the Turkey Point station, which are elevated above the existing grade, are not inundated and remain dry. The inundation of the area surrounding the site of Units 6 & 7 is not caused by the Florida Escarpment tsunami. It is a consequence of the assumption regarding the initial sea water level that accounts for the 10 percent exceedance high tide level of 3.6 feet mean low water (MLW), initial rise of 0.9 feet and long term sea level rise of 1.0 foot, the sum of which produces an initial water level, i.e., prior to the arrival of the tsunami, equal to 1.68 meters (5.5 feet) MLW, or 3.6 feet (1.10 meters) NAVD 88. This initial water level is enough to inundate a large zone along the Florida coast, including the area around Units 6 & 7. This is made clear in Figure 17, which shows the water depth over the area of Grid C relative to the two different levels of the water surface. Figure 17(a) shows the water depth relative to MLW without the water level rise that is used to define the initial condition for the tsunami propagation simulations. Figure 17(b) shows the water depth relative to the assumed initial water surface in the Florida Escarpment tsunami simulations, i.e., relative to 10 percent exceedance high tide + initial rise + long-term sea level rise. As can be seen in Figure 17(b), the area surrounding the site of Units 6 & 7 and its vicinity are inundated even prior to the arrival of the tsunami, i.e., under the assumed initial condition for the tsunami propagation simulations. Again, the Units 6 & 7 site itself and other parts of the Turkey Point station, which are elevated above the existing grade, are not inundated and remain dry. Figure 18 shows the maximum water surface rise in the vicinity of the Units 6 & 7, relative to the initial sea water level. The maximum water surface level rise over the entire area shown in Figure 18 is very small, less than 0.07 meters.

Figure 19 shows the water level at Units 6 & 7 from the dynamic source simulation as a function of time. The maximum water surface level rise caused by the Florida Escarpment tsunami is less than 0.02 meters over the initial water level, occurring after four hours from the initiation of the Florida Escarpment slide, and about an hour and a half after the arrival of the first waves caused by the Florida Escarpment tsunami. The predicted maximum water surface level is 1.71 meters (5.6 feet) MLW, or 3.7 feet (1.14 meters) NAVD 88.

Static Source Initial Condition

Figure 21 and Figure 22 show the propagation of the tsunami wave generated by a static source over the domain of Grid A during the first 160 minutes, presenting snapshots of the wave height every 20 minutes. As is seen in these figures, the tsunami propagation pattern is similar to that in the dynamic source simulation, but the wave heights away from the source towards the west are much smaller than those for the dynamic sources shown in Figure 8. The wave propagation to the east towards Florida is quite similar as that simulated with a dynamic source.

This is illustrated in Figure 23, which shows the maximum water surface elevation within the model domain of Grid A during the simulation period. Comparing Figure 23 with Figure 10 shows that the static source produces smaller water surface levels to the west of the source, but similar water levels to the east. This could be attributed to the fact that in the case of the dynamic source the initial condition entered in FUNWAVE-TVD includes the velocities obtained with NHWAVE, while in the case of the static source the initial velocities in the vicinity of the source are zero. Assigning a velocity to the initial wave in the dynamic source case results in a higher total energy than in the static source case where the initial velocity is assumed to be zero. In the area right over the slide and its immediate vicinity to the west the maximum water surface levels obtained with the static source are higher than those obtained with the dynamic source.

Figure 24 and Figure 25 show the propagation of the tsunami wave in Grid B, from 80 minutes in the FUNWAVE-TVD simulation and after the wave enters the Grid B domain, until 240 minutes. Snapshots of the wave height every 20 minutes are shown. Figure 26 shows the maximum water surface elevation within the model domain of Grid B during the simulation period. The predicted water surface levels in Grid B for the static source are quite similar to those for the dynamic source shown in Figure 11, Figure 12, and Figure 13.

Figure 27 and Figure 28 show the propagation of the tsunami wave in Grid C, from 140 minutes until 240 minutes in the FUNWAVE-TVD simulation. Snapshots of the wave height every 20 minutes are shown. Figure 29 shows the maximum water level over Grid C. Again the predicted water surface elevations over Grid C for the static source are quite similar to those predicted with a dynamic source, shown in Figure 14 and Figure 15.

Figure 30 shows the maximum water surface rise in the vicinity of the Turkey Point Units 6 & 7, relative to the initial sea water level. Figure 31 shows the water level near Units 6 & 7 from the static source simulation as a function of time. The maximum water surface level rise caused by the Florida Escarpment tsunami is 0.02 meters, occurring after four hours from the initiation the Florida Escarpment slide, and about one hour and a half after the arrival of the first waves caused by the Florida Escarpment tsunami. The maximum water level near Units 6 & 7 predicted with the static source is the same as that predicted using a dynamic source, i.e., 1.71 meters (5.6 feet) MLW, or 3.7 feet (1.14 meters) NAVD 88.

Summary of Results

A literature review was performed to identify the characteristics of a potential future submarine slope failure near the Florida Straits. Conservative assumptions were made to define such a submarine slide as a source of a tsunami event. The postulated slide was equal to the maximum credible submarine slide above the Florida Escarpment, developed from multibeam bathymetric data and outlined in Reference 7. The slide area was schematized as having a shape similar to that described in Reference 8, i.e., as having an elliptical base with its minor and major axes equal to the length and width of the slide area, 19.2 kilometers (in the direction of motion), 42.9 kilometers respectively. The maximum thickness of the schematized slide was 66 meters.

Simulations with two alternative initial conditions (dynamic and static) for the water surface at the onset of the tsunami event were made. In both cases the assumed initial sea water level includes the 10 percent exceedance high tide, an initial rise plus the long-term sea level rise, all of which add up to 1.68 meters (5.5 feet) MLW, 3.6 feet (1.11 meters) NAVD

88, same as that used for the PMT numerical simulation in FSAR 2.4.6.4 and for the probable maximum storm surge evaluation as explained in FSAR 2.4.5.2.2.1. This antecedent condition leads to inundation of large parts of southeast Florida, including the area surrounding the site of Units 6 & 7 even prior to the arrival of the Florida Escarpment tsunami. The Units 6 & 7 site itself and other parts of the Turkey Point station, which are elevated above the existing grade, are not inundated and remain dry.

First, the non-hydrostatic code NHWAVE was used to simulate the motion of the slide and simulate the water surface elevation and horizontal velocities. The computed water surface and velocities were used as the dynamic source initial conditions in the simulation of the tsunami propagation with the Boussinesq code FUNWAVE-TVD. The initial maximum wave and negative (depression) wave produced by NHWAVE were 47.2 meters and –77.5 meters respectively. The propagation of the tsunami was simulated through three nested grids (Grid A, Grid B and Grid C), each of which provided finer grid resolution. The simulation suggests that the relative water surface rise at Units 6 & 7 due to the Florida Escarpment slide is small. The predicted maximum water sea level rise at Turkey Point caused by the Florida Escarpment tsunami was 0.02 meters, or 0.1 feet above the initial ocean water level.

Secondly, a static source approach was used. In this case the initial condition for the tsunami wave was assumed to be a dipole with a depression and a rise of water levels having the shape of the displaced mass of the submarine failure. The initial water surface condition for the FUNWAVE-TVD simulations includes a 66-meter depression of the water surface over the slide and a 66-meter rise downslope of the slide. The initial velocity field in this case is zero. The predicted water levels with the static source are lower to the east and southeast, but higher over the slide area and its vicinity to the west. The predicted water levels near Units 6 & 7 were quite similar to those obtained with the dynamic source. The predicted maximum water sea level rise near Units 6 & 7 caused by the Florida Escarpment tsunami was 0.02 meter (0.1 feet) above the initial ocean water level.

Conclusions

Simulations of a tsunami generated by a conservatively large submarine mass failure along the Florida Escarpment suggest that the impact of such an event on water levels near Units 6 & 7 will be very small. The maximum predicted water level near Units 6 & 7 due to this tsunami event will be 1.71 meters (5.6 feet) MLW, or 3.7 feet (1.14 meters) NAVD 88, representing a rise of only 0.02 meters above the initial sea water level. The assumed initial sea water level in the FUNWAVE model simulation includes the 10 percent exceedance high tide, an initial rise plus the long-term sea level rise, all of which add up to 1.68 meters (5.5 feet) MLW or 3.6 feet (1.11 meters) NAVD 88. This water level is much smaller than the maximum tsunami water level of 4.5 meters MSL (4.82 meters MLW) reported for the PMT case in FSAR Subsection 2.4.6.5. This conclusion is also consistent with the results of the Florida Escarpment Slide evaluation described in FSAR 2.4.6.1.2.

Figure 1. (a) Morphology of the West Florida Escarpment and West Florida Slope, and (b) extent and distribution of carbonate debris flow deposits and talus deposits. "Tertiary failures" marks the general location of older landslides mapped by Mullins et al (Reference 3) that now have been completely buried. Inset box shows a detailed view of some of the carbonate talus deposits (Source: Reference 7).

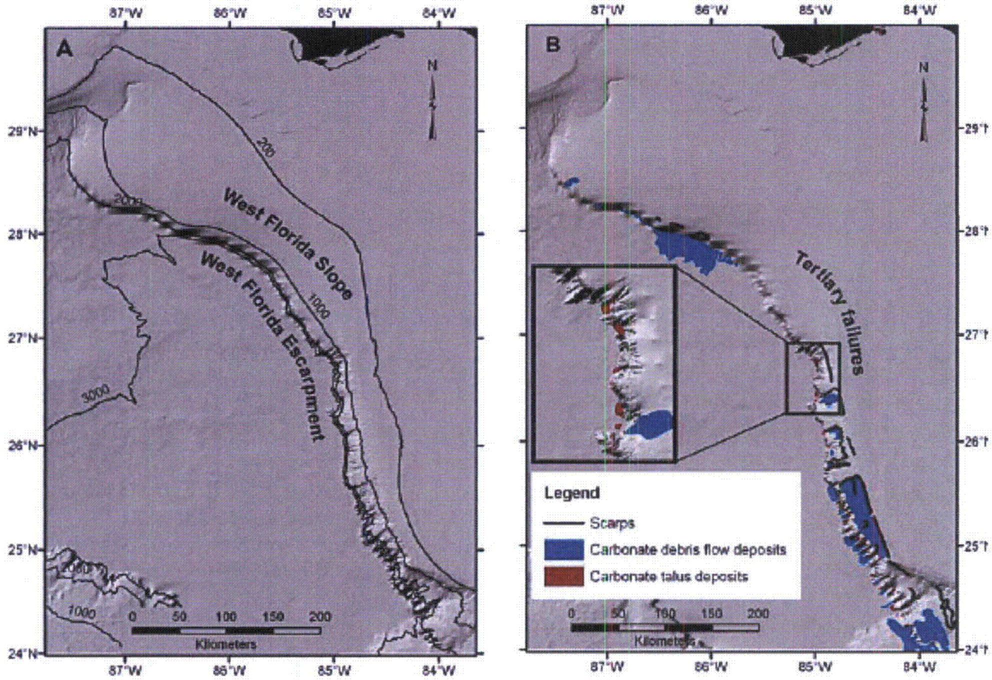

(a) (b)

Figure 2. Outline of maximum credible submarine slide above the Florida Escarpment, developed from multibeam bathymetric data (Source: Reference 7).

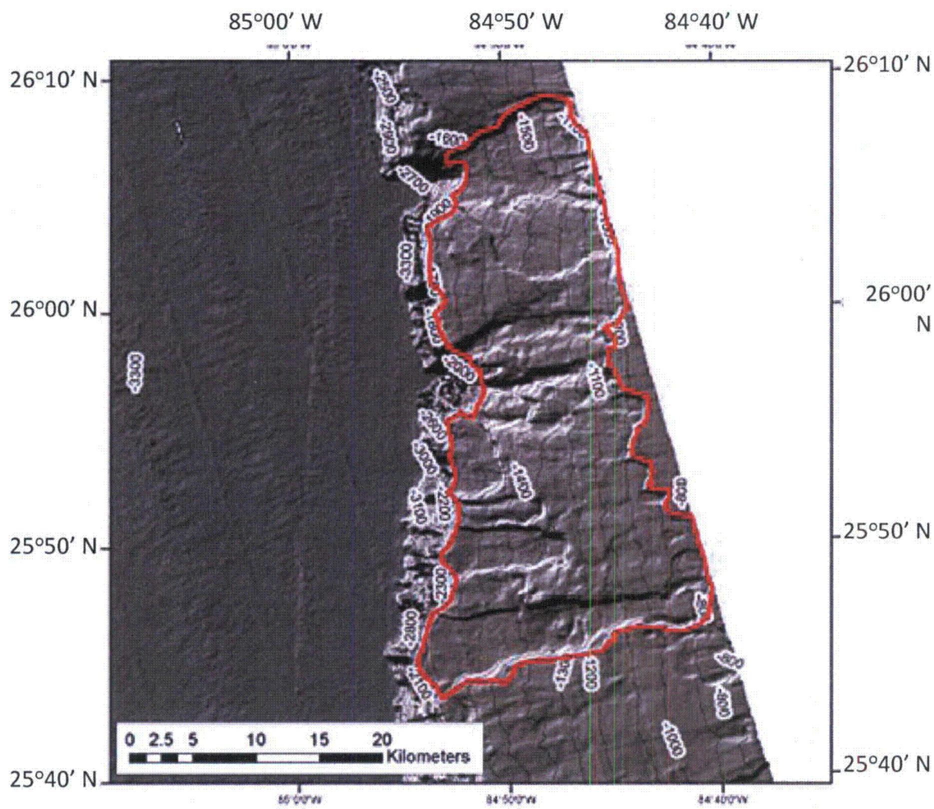

Figure 3. Approximation of the maximum credible submarine slide above the Florida Escarpment with an ellipse. (Source of bathymetry: Reference 7).

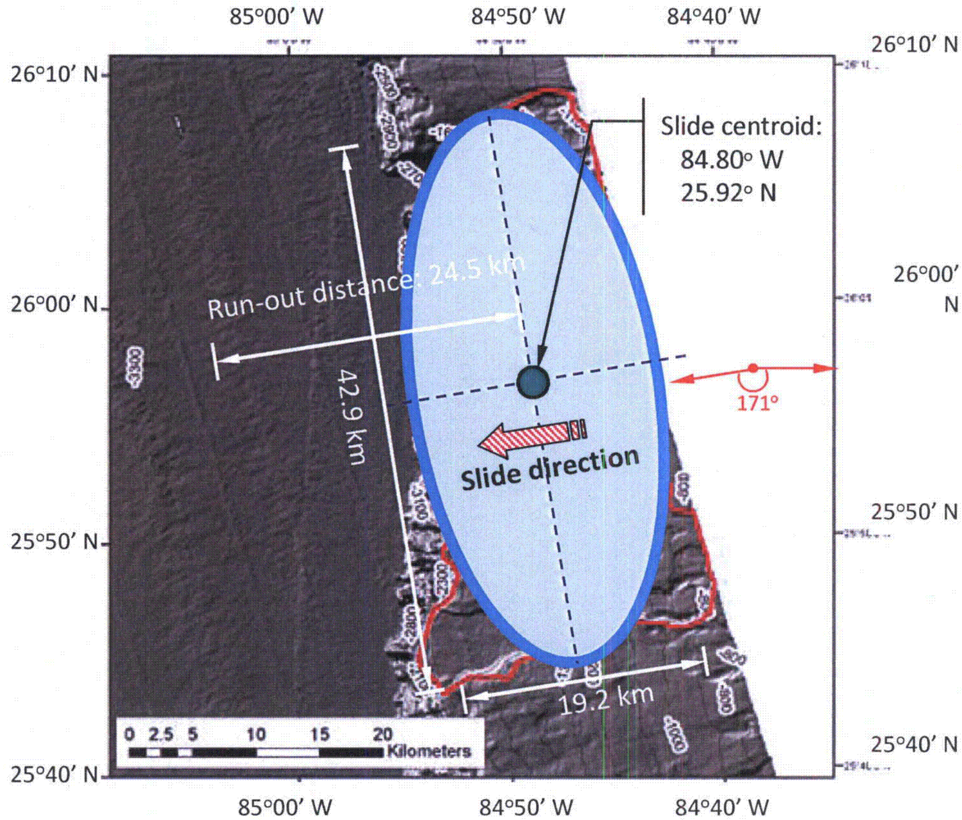

Figure 4. Model domain and bathymetry in the three nested grids used in the FUNWAVE simulations. Colors in elevation legend represent water depths in meters relative to MSL for ETOPO1 data (Reference 16) and MLW for Coastal Relief Model data (Reference 17).

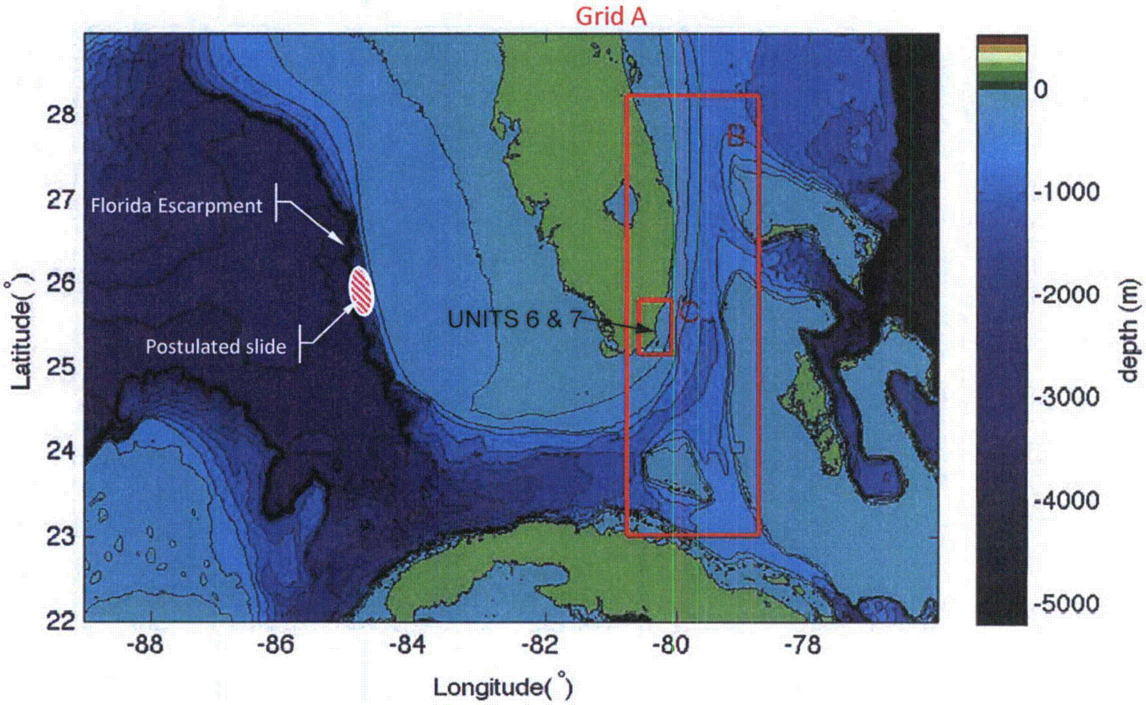

Figure 5. Location and lateral extent of the postulated submarine mass failure for the Florida Escarpment slide simulations and local bathymetry. Colors in elevation legend represent water depths relative to MLW in meters (Source: Reference 17).

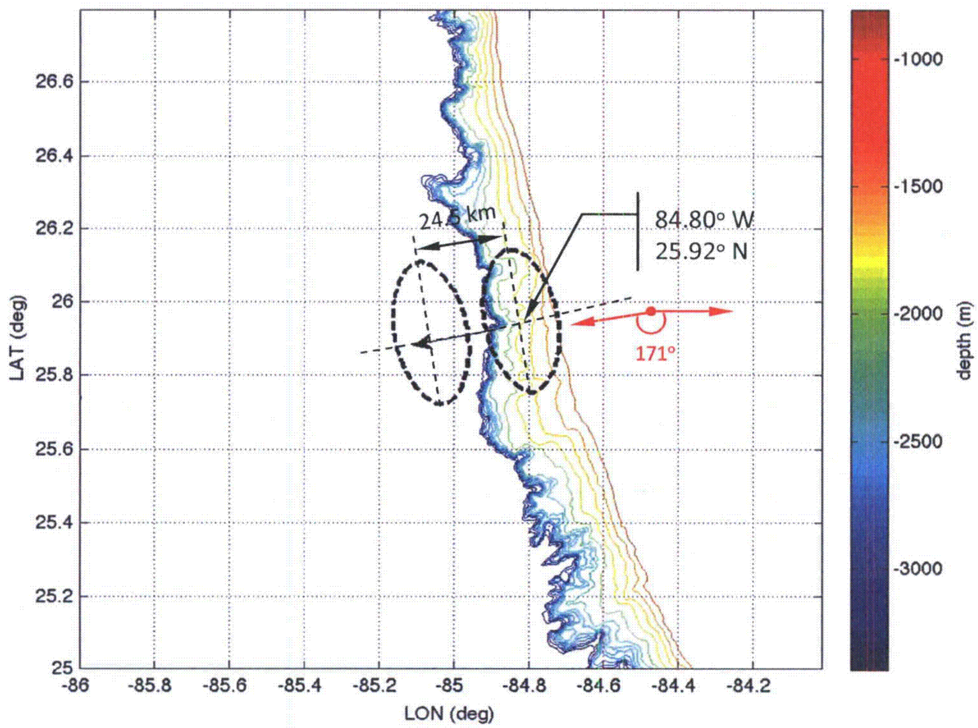

Figure 6. Initial wave generated by NHWAVE (dynamic source) for the Florida Escarpment submarine failure. Colors in elevation legend indicate water surface elevation (MLW) in meters. Bathymetry contours indicate water depths (MLW) in meters.

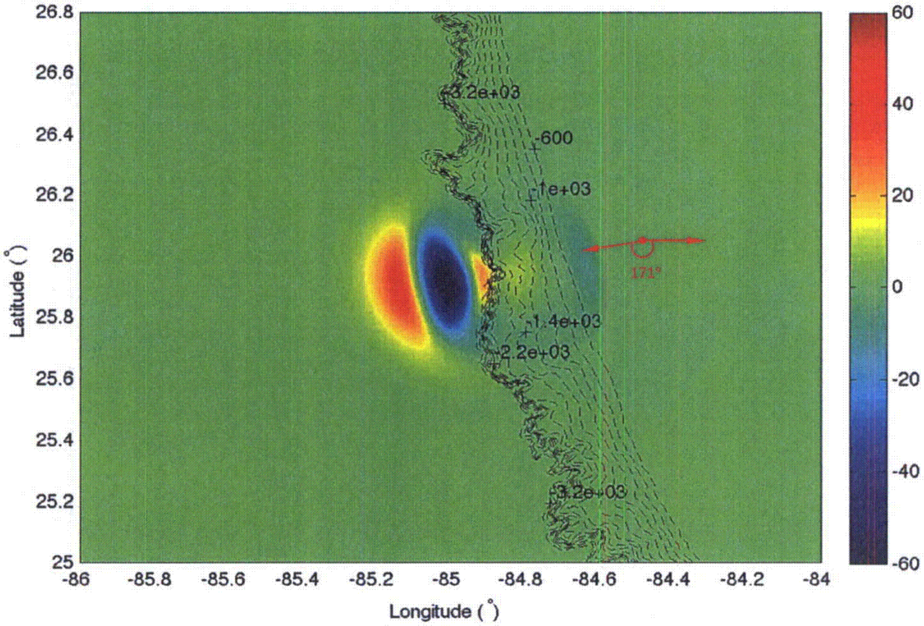

Figure 7. (a) Water surface profiles in the direction of the slide motion at different times after the initiation of the slide obtained from NHWAVE and (b) ocean floor profile. The water surface profiles and cross section shown in this Figure are along the minor axis of the ellipse shown in Figure 3.

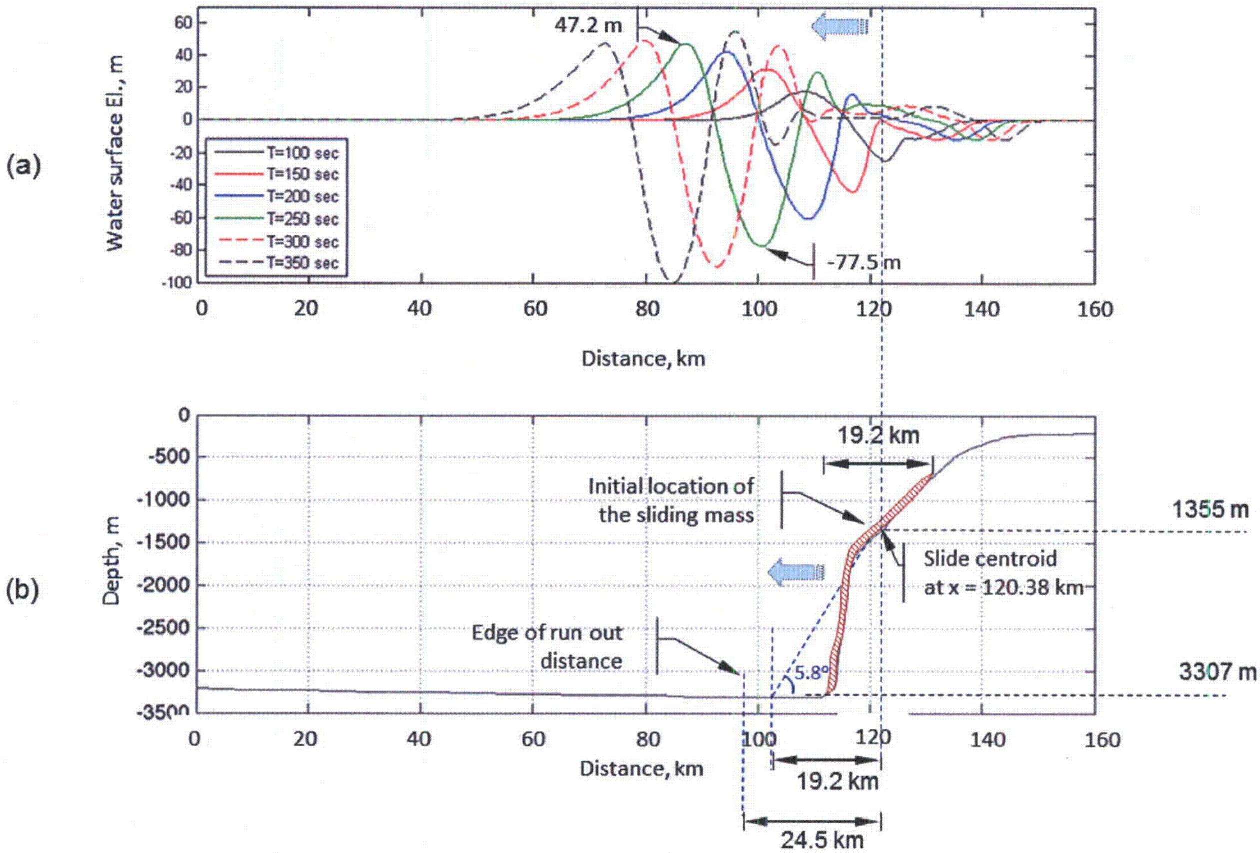

Figure 8. Simulated propagation of the Florida Escarpment tsunami (dynamic source) in Grid A at 0, 20, 40, 60, 80, and 100 minutes after the submarine mass failure. Colors in elevation legend represent water surface elevations in meters relative to MSL for ETOPO1 data (Reference 16) and MLW for Coastal Relief Model data (Reference 17).

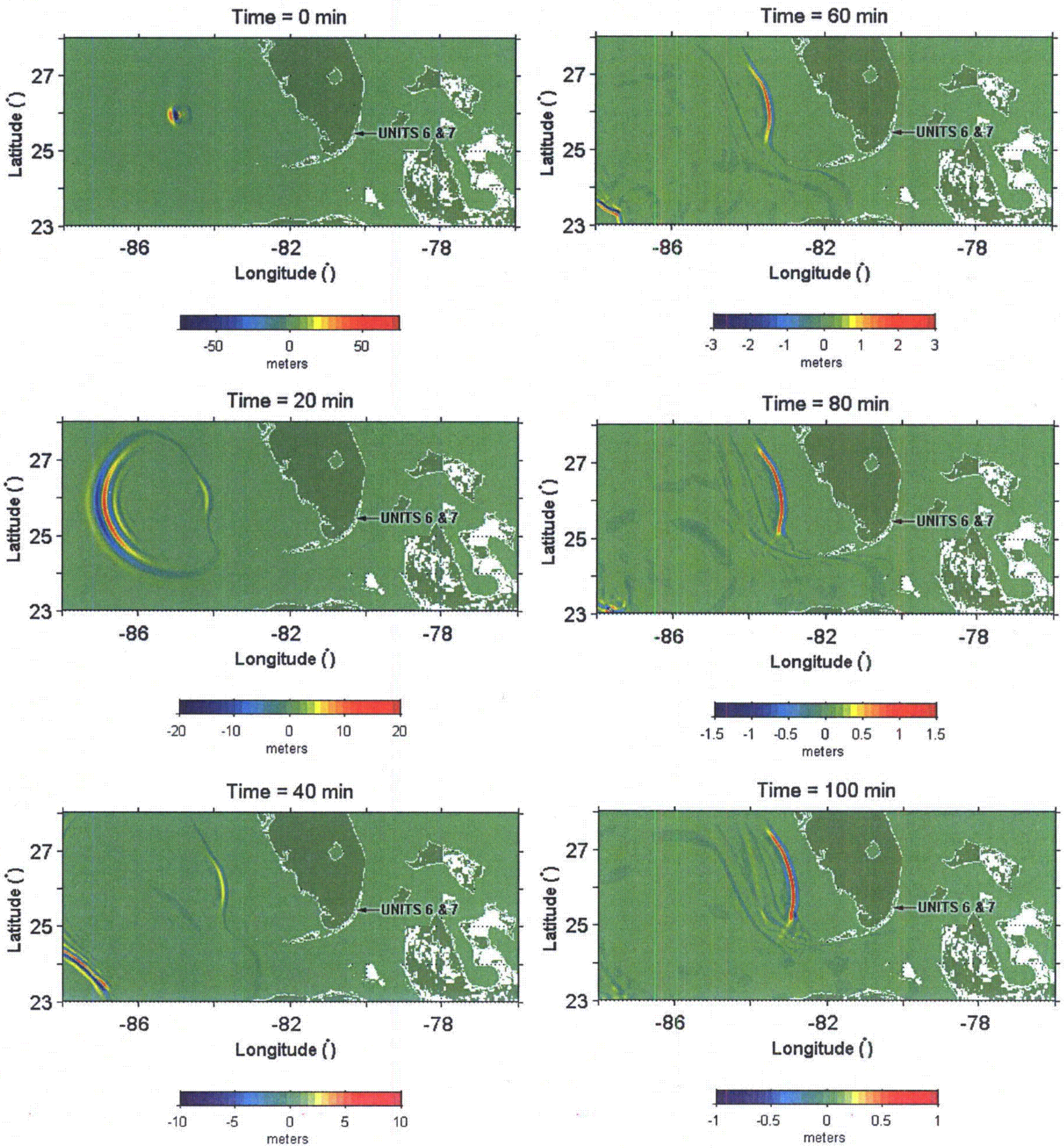

Figure 9. Simulated propagation of the Florida Escarpment tsunami (dynamic source) in Grid A at 120, 140, 160, and 180 minutes after the submarine mass failure. Colors in elevation legend represent water surface elevations in meters relative to MSL for ETOPO1 data (Reference 16) and MLW for Coastal Relief Model data (Reference 17).

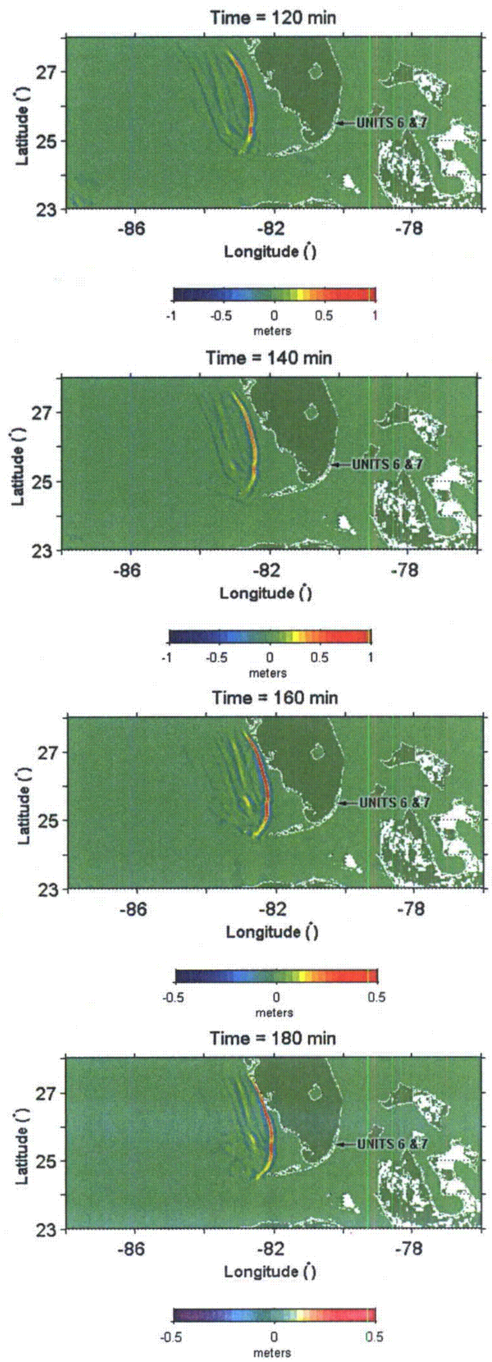

Figure 10. Simulated maximum wave height during the propagation of the Florida Escarpment tsunami (dynamic source) in Grid A. Colors in elevation legend represent water surface elevations in meters relative to MSL for ETOPO1 data (Reference 16) and MLW for Coastal Relief Model data (Reference 17).

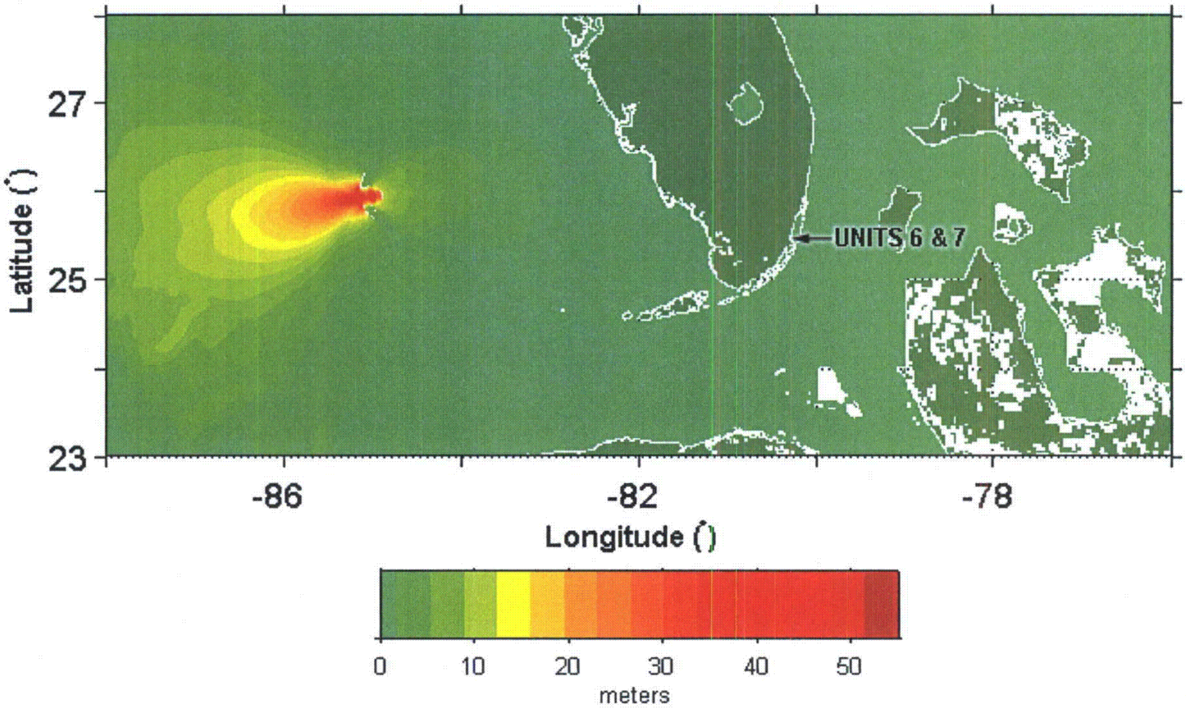

Figure 11. Simulated propagation of the Florida Escarpment tsunami (dynamic source) in Grid B at 80, 100, 120, 140, 160, and 180 minutes after the submarine mass failure. Colors in elevation legend represent water surface elevations in meters relative to MSL for ETOPO1 data (Reference 16) and MLW for Coastal Relief Model data (Reference 17).

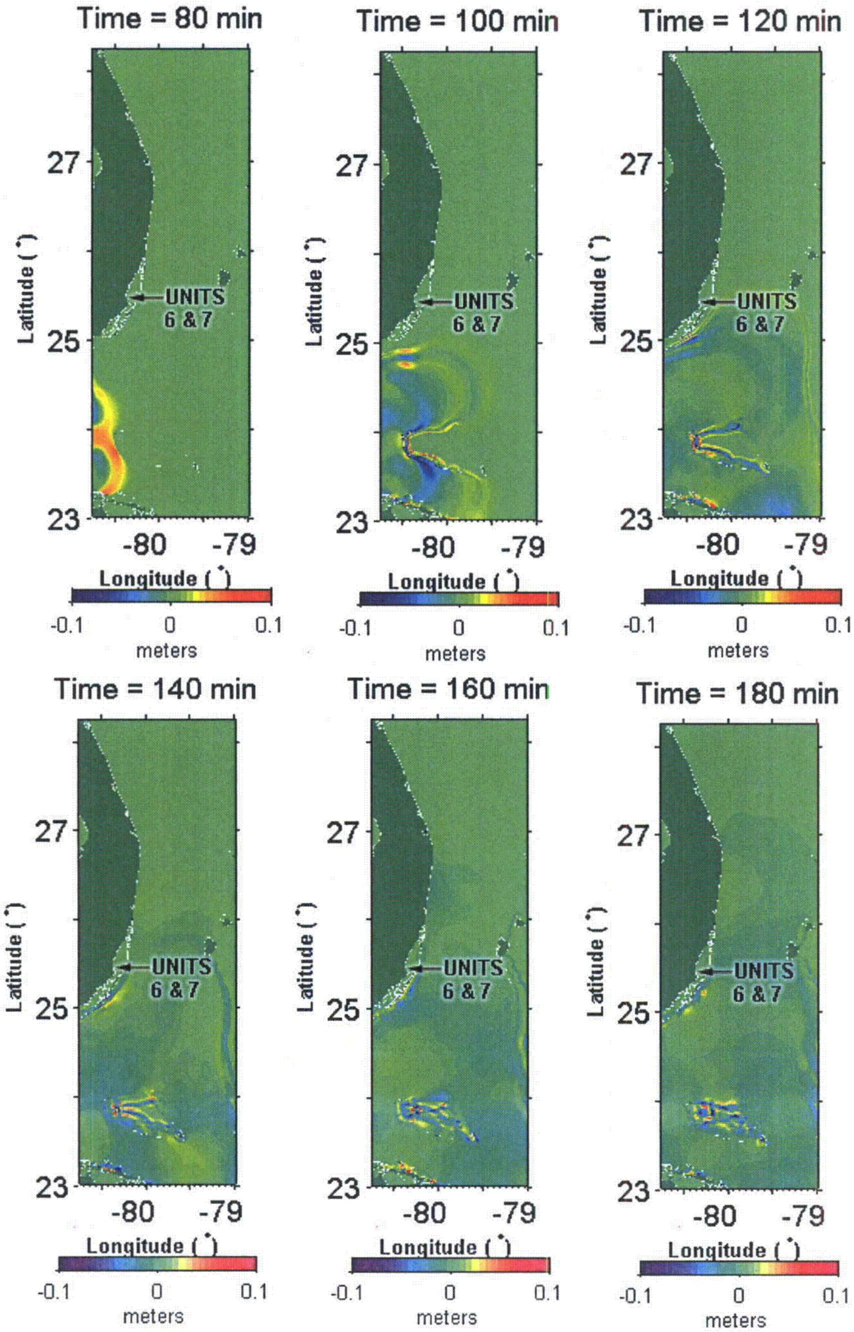

Figure 12. Simulated propagation of the Florida Escarpment tsunami (dynamic source) in Grid B at 200, 220, and 240 minutes after the submarine mass failure. Colors in elevation legend represent water surface elevations in meters relative to MSL for ETOPO1 data (Reference 16) and MLW for Coastal Relief Model data (Reference 17).

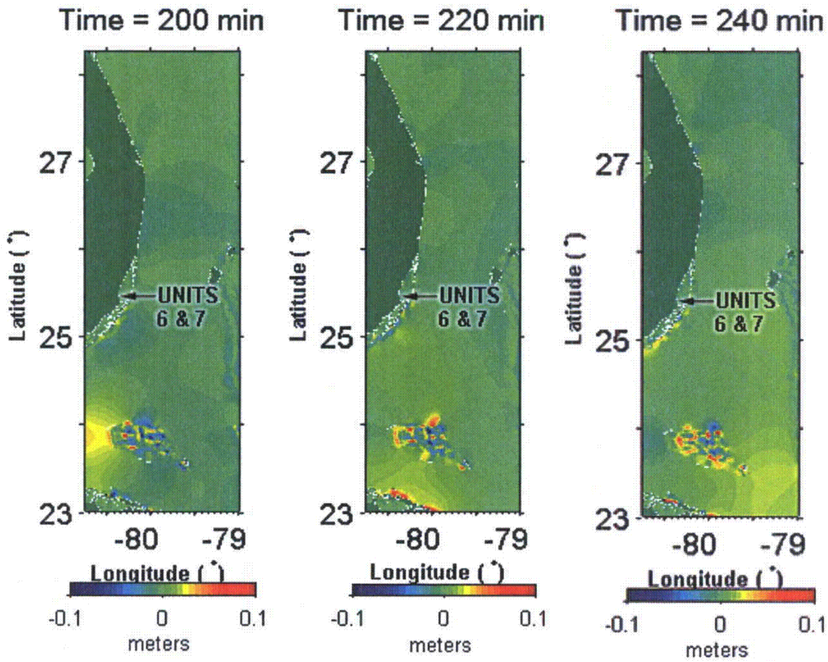

Figure 13. Simulated maximum wave height during the propagation of the Florida Escarpment tsunami (dynamic source) in Grid B. Colors in elevation legend represent water surface elevations in meters relative to MSL for ETOPO1 data (Reference 16) and MLW for Coastal Relief Model data (Reference 17).

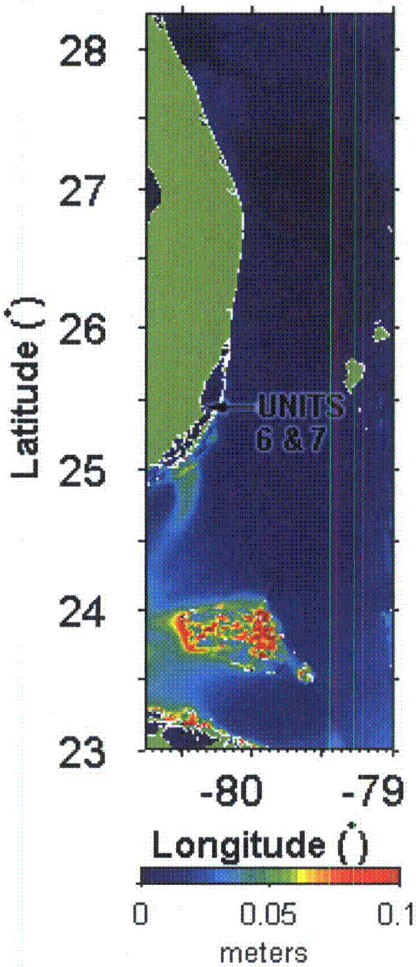

Figure 14. Simulated propagation of the Florida Escarpment tsunami (dynamic source) in Grid C at 140, 160, 180, and 200 minutes after the submarine failure. Colors in elevation legend represent water surface elevations relative to MLW in meters.

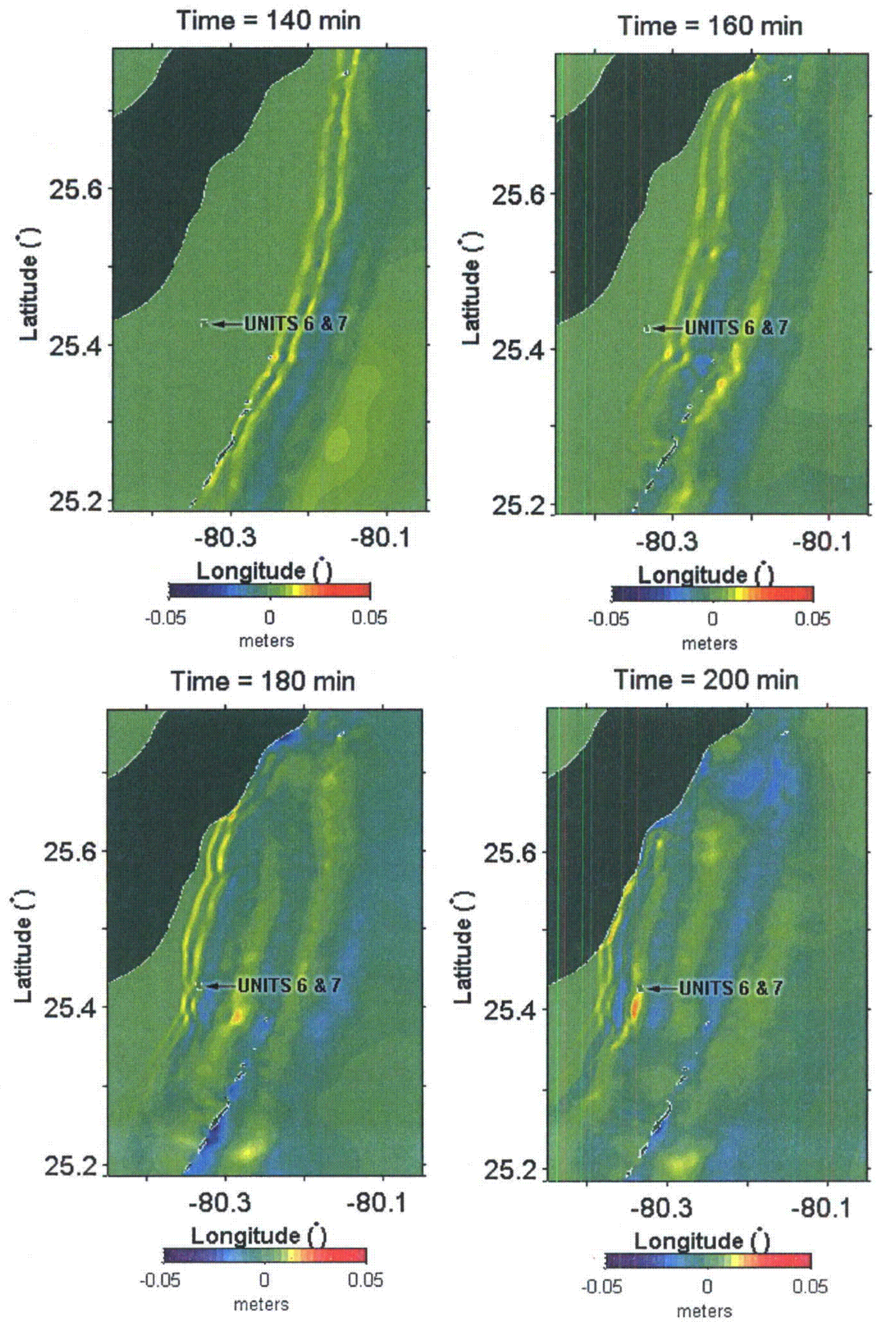

Figure 15. Simulated propagation of the Florida Escarpment tsunami (dynamic source) in Grid C at 220 and 240 minutes after the submarine failure. Colors in elevation legend represent water surface elevations relative to MLW in meters.

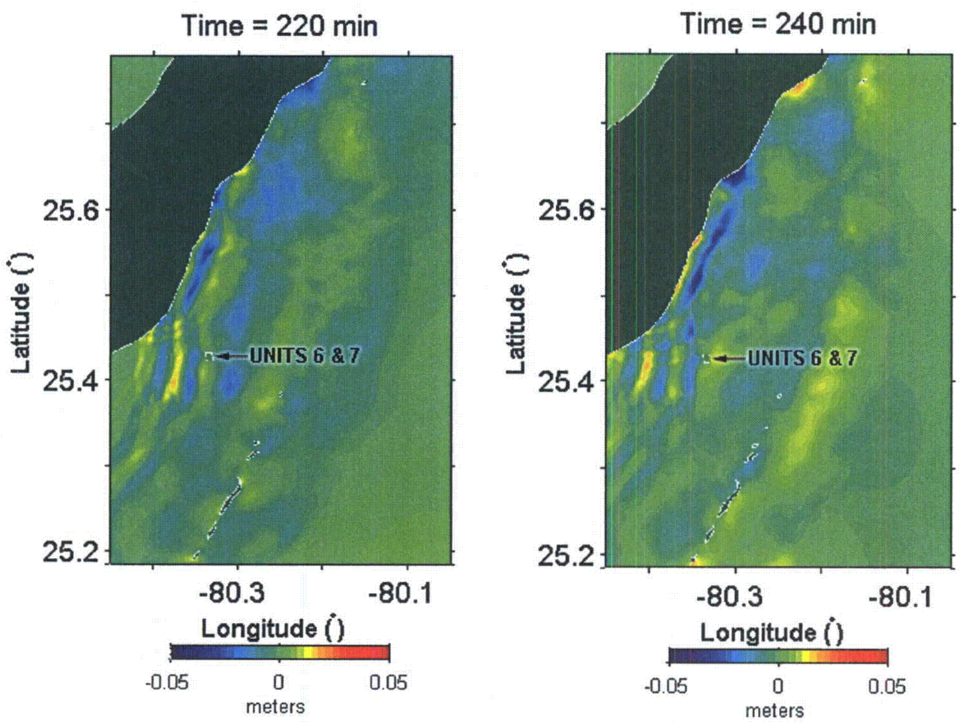

Figure 16. Simulated maximum water surface elevation during the propagation of the Florida Escarpment tsunami (dynamic source) in Grid C. Colors in elevation legend represent water surface elevations relative to MLW in meters.

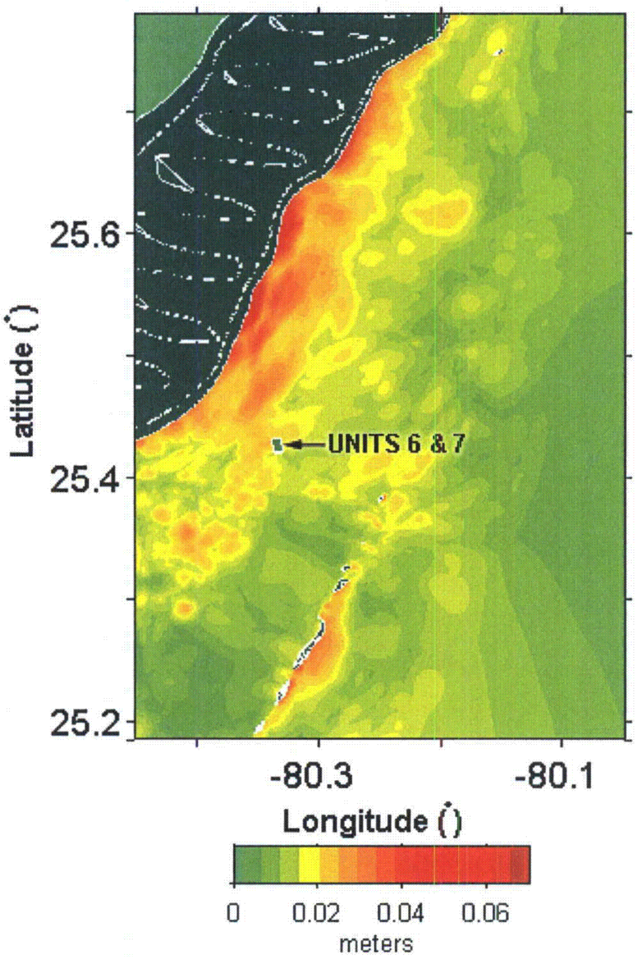

Figure 17. (a) Water depth relative to MLW over the area of Grid C without the water level rise that is used to define the initial condition for the tsunami propagation simulations; and (b) water depth relative to the assumed initial water surface in the Florida Escarpment tsunami simulations, i.e., 10 percent exceedance high tide + initial sea rise + long-term sea level rise. Colors in elevation legend represent depths relative to MLW in meters.

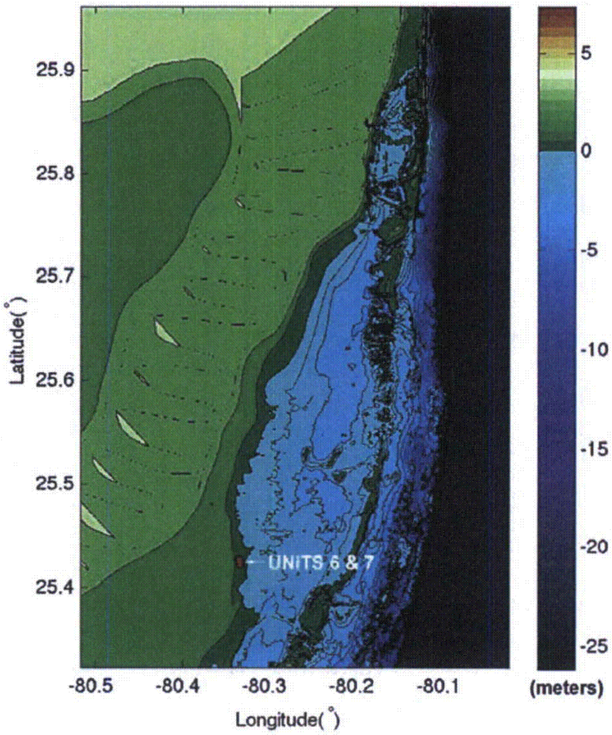

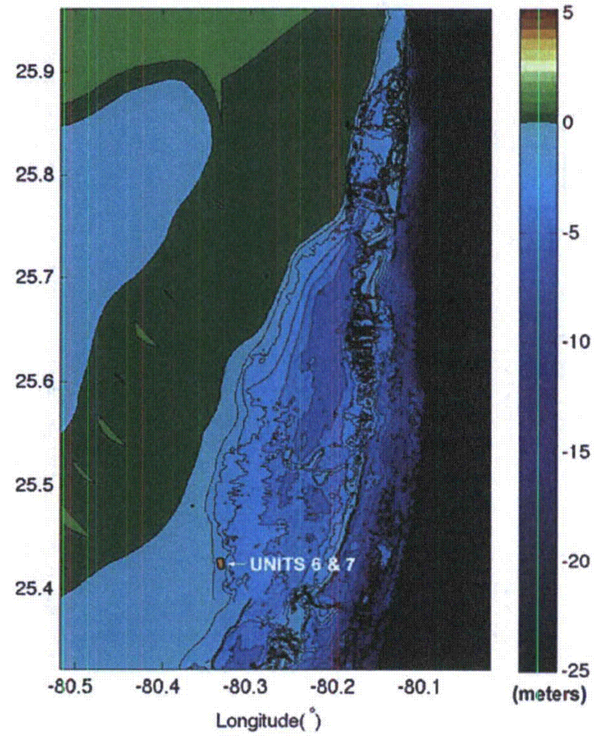

Figure 18. Simulated maximum water surface rise, relative to the initial sea water level, during the propagation of the Florida Escarpment tsunami (dynamic source) in the vicinity of Units 6 & 7. Colors in elevation legend represent water surface elevations relative to MLW in meters.

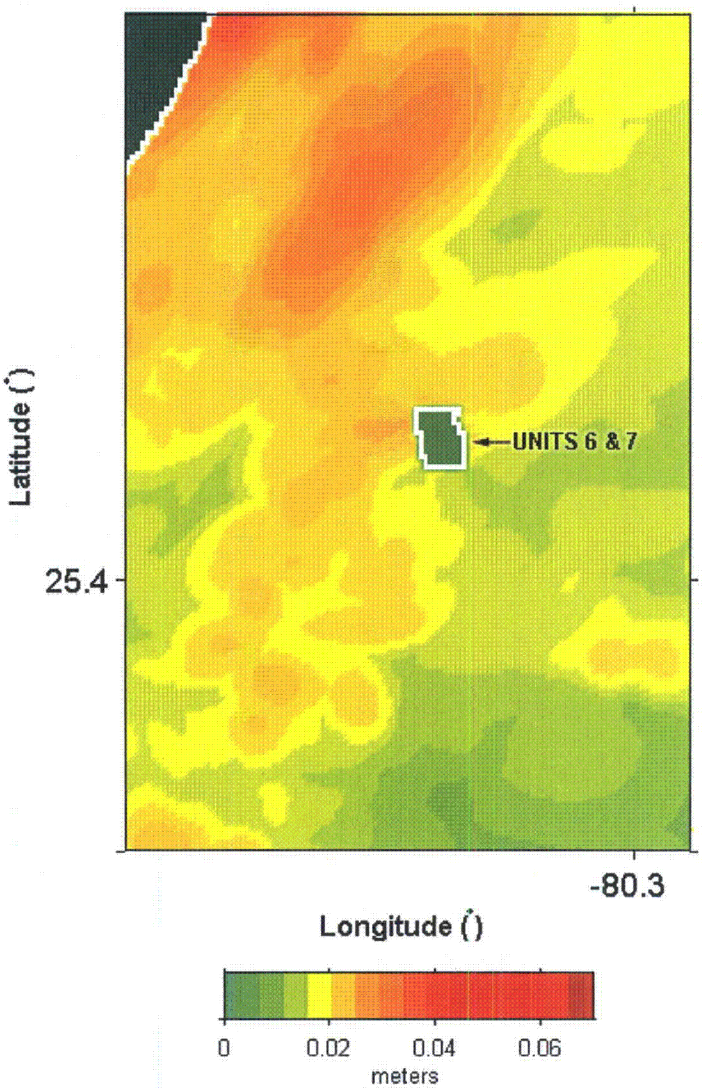

Figure 19. Water surface elevation at the FPL Turkey Point Units 6 & 7 as a function of time following the Florida Escarpment tsunami (dynamic source). Water surface elevations are relative to the initial water level.

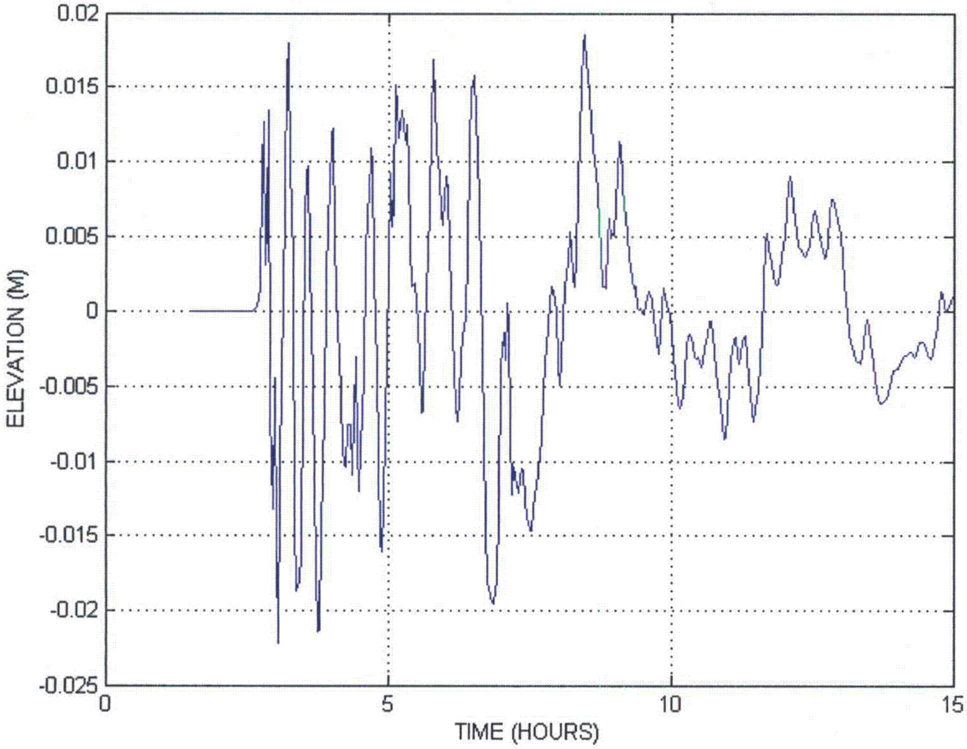

Figure 20. Initial water surface wave for a static source representation of the Florida Escarpment submarine failure shown in Figure 3. Colors in elevation legend indicate water surface elevation (MLW) in meters. Bathymetry contours indicate water depths (MLW) in meters.

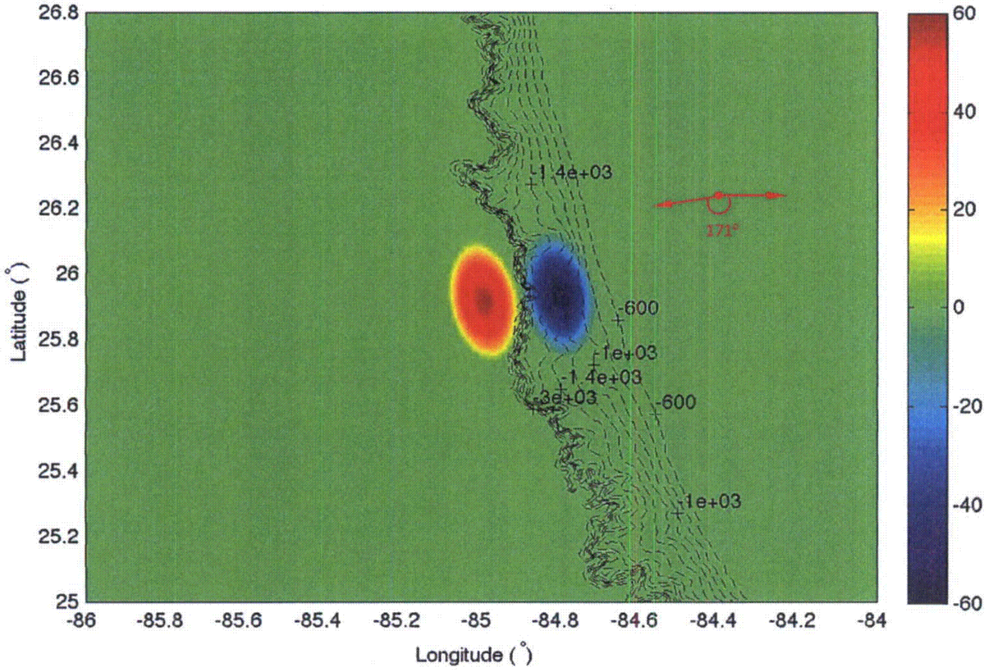

Figure 21. Simulated propagation of the Florida Escarpment tsunami (static source) in Grid A at 0, 20, 40, 60, 80 and 100 minutes after the submarine failure. Colors in elevation legend represent water surface elevations in meters relative to MSL for ETOPO1 data (Reference 16) and MLW for Coastal Relief Model data (Reference 17).

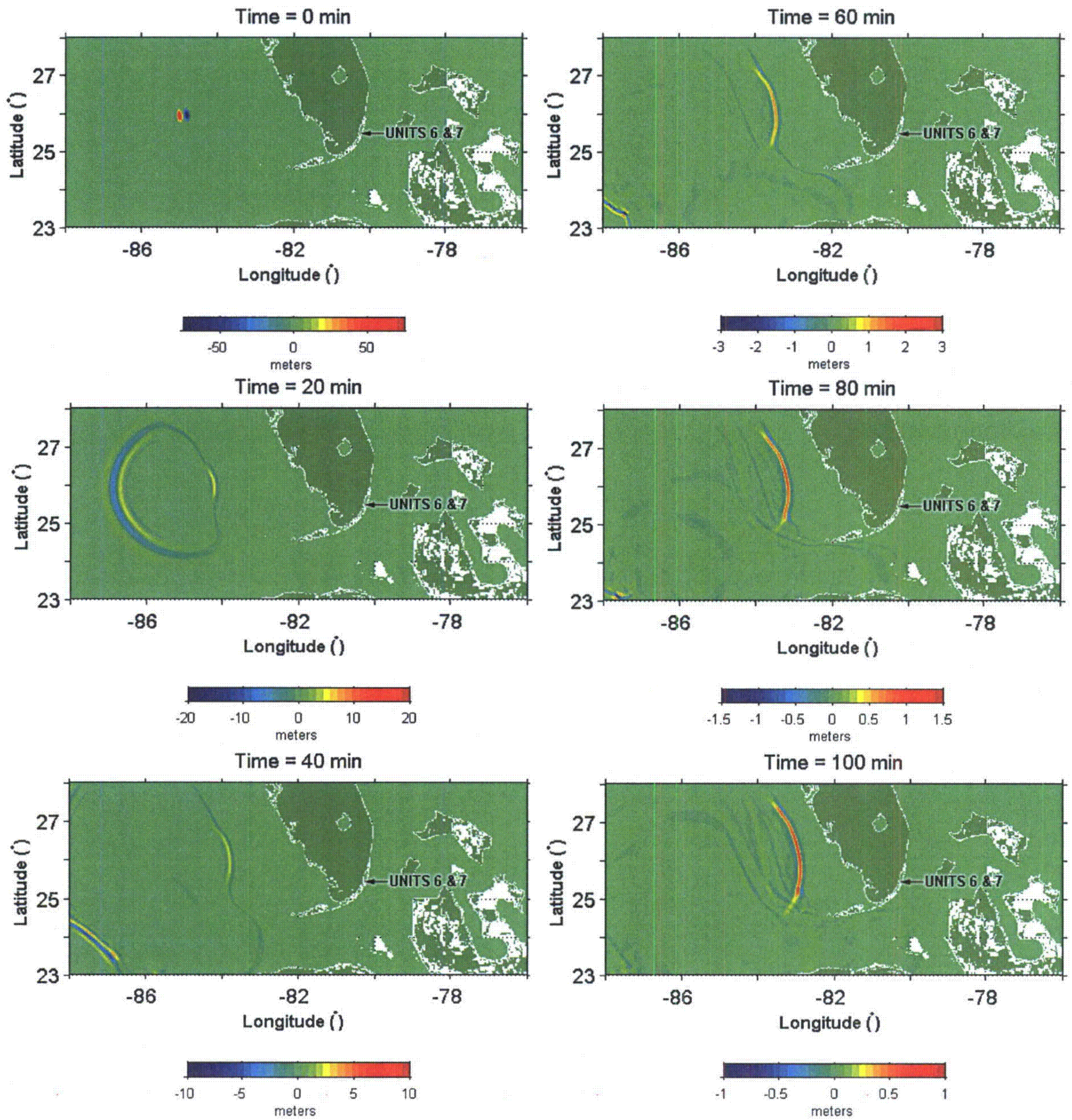

Figure 22. Simulated propagation of the Florida Escarpment tsunami (static source) in Grid A at 120, 140, 160, and 180 minutes after the submarine failure. Colors in elevation legend represent water surface elevations in meters relative to MSL for ETOPO1 data (Reference 16) and MLW for Coastal Relief Model data (Reference 17).

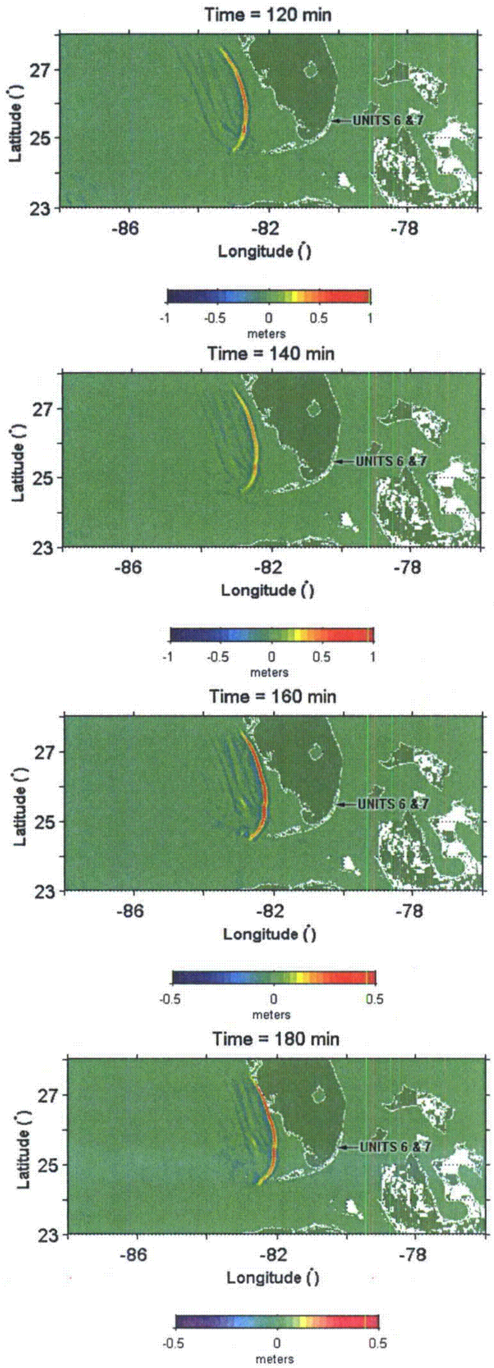

Figure 23. Simulated maximum water surface elevation during the propagation of the Florida Escarpment tsunami (static source) in Grid A. Colors in elevation legend represent water surface elevations in meters relative to MSL for ETOPO1 data (Reference 16) and MLW for Coastal Relief Model data (Reference 17).

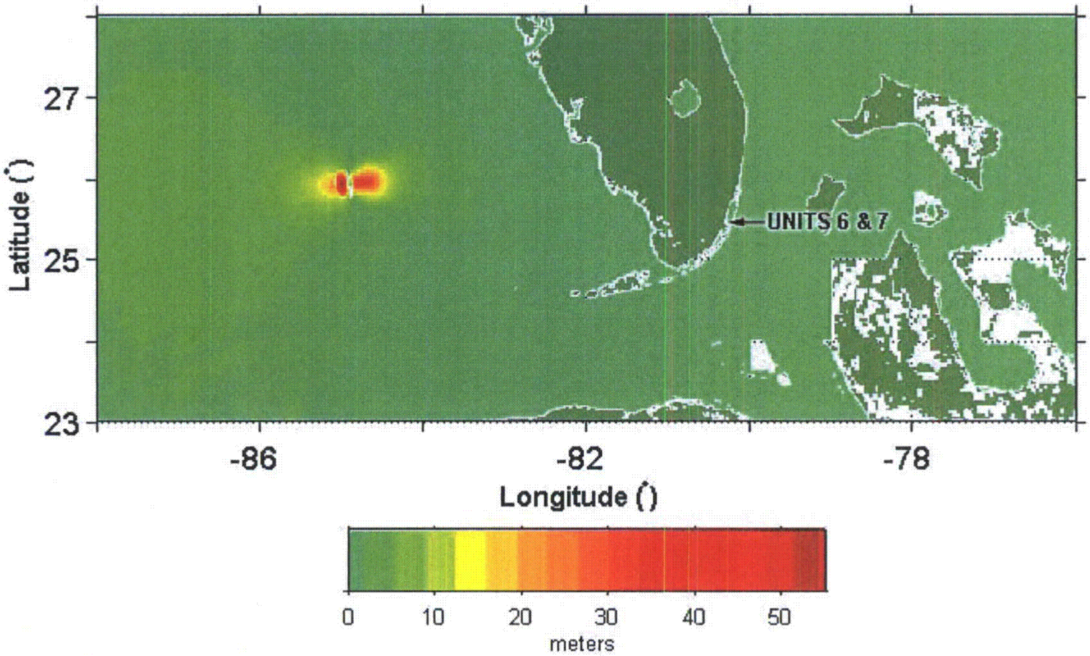

Figure 24. Simulated propagation of the Florida Escarpment tsunami (static source) in Grid B at 80, 100, 120, 140, 160, and 180 minutes after the submarine failure. Colors in elevation legend represent water surface elevations in meters relative to MSL for ETOPO1 data (Reference 16) and MLW for Coastal Relief Model data (Reference 17).

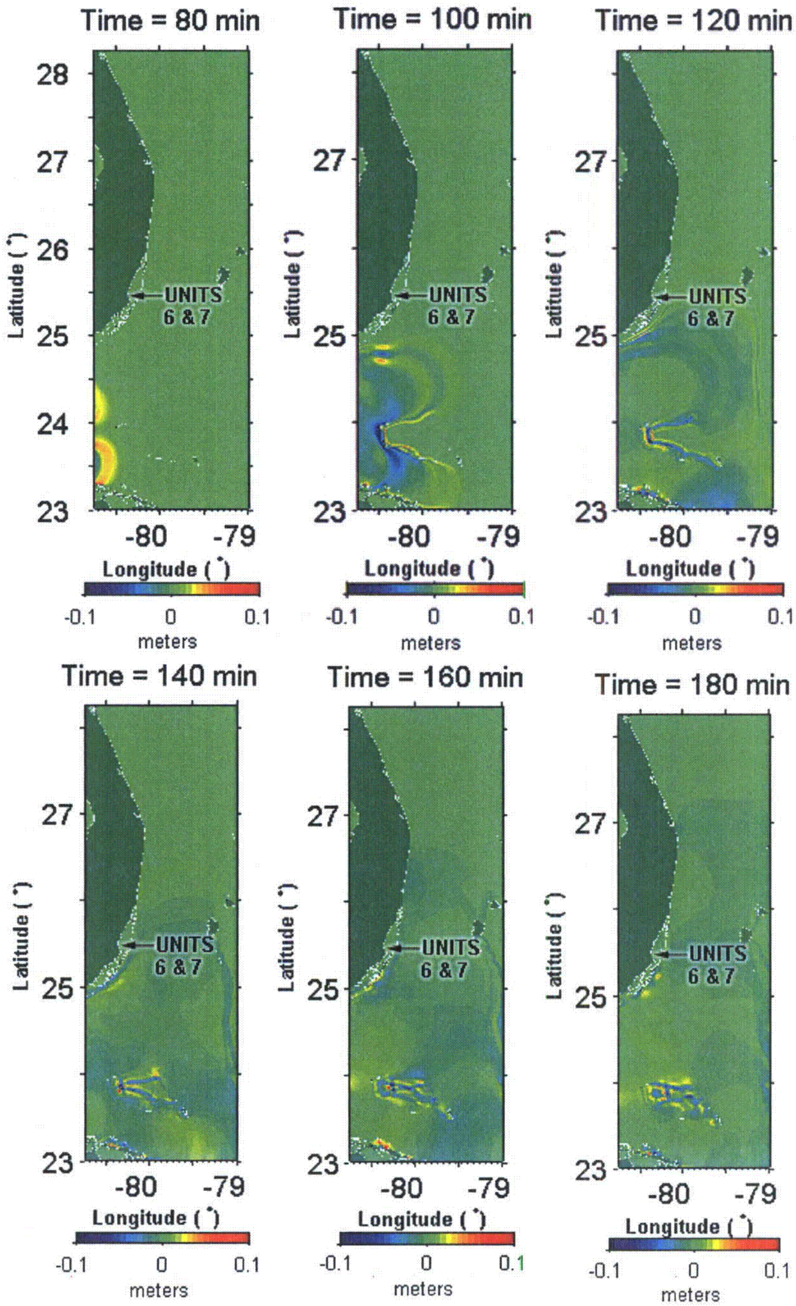

Figure 25. Simulated propagation of the Florida Escarpment tsunami (static source) in Grid B at 200, 220, and 240 minutes after the submarine failure. Colors in elevation legend represent water surface elevations in meters relative to MSL for ETOPO1 data (Reference 16) and MLW for Coastal Relief Model data (Reference 17).

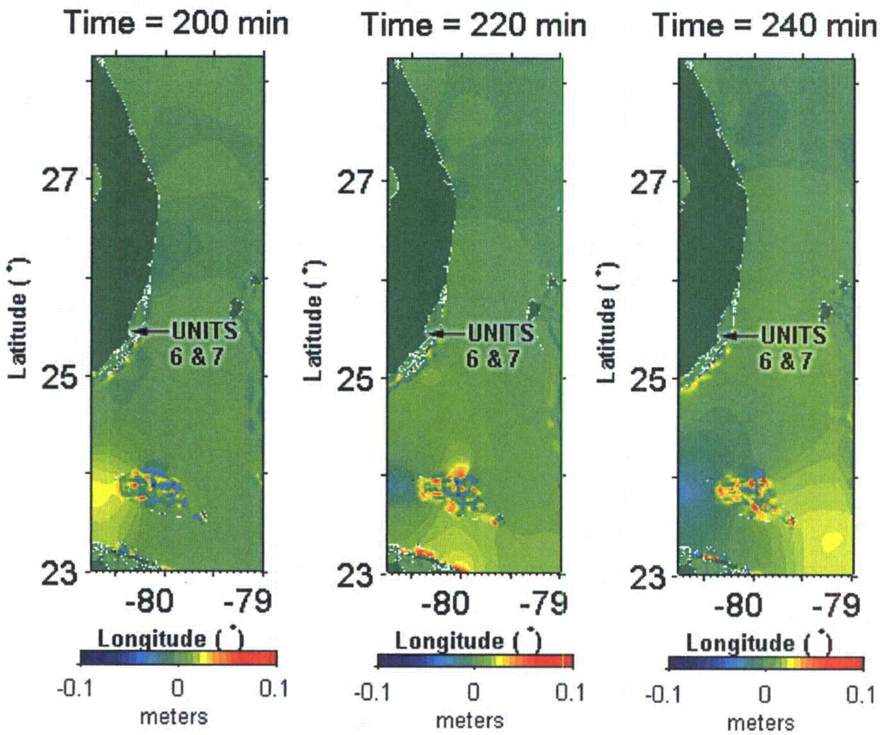

Figure 26. Simulated maximum water surface elevation during the propagation of the Florida Escarpment tsunami (static source) in Grid B. Colors in elevation legend represent water surface elevations in meters relative to MSL for ETOPO1 data (Reference 16) and MLW for Coastal Relief Model data (Reference 17).

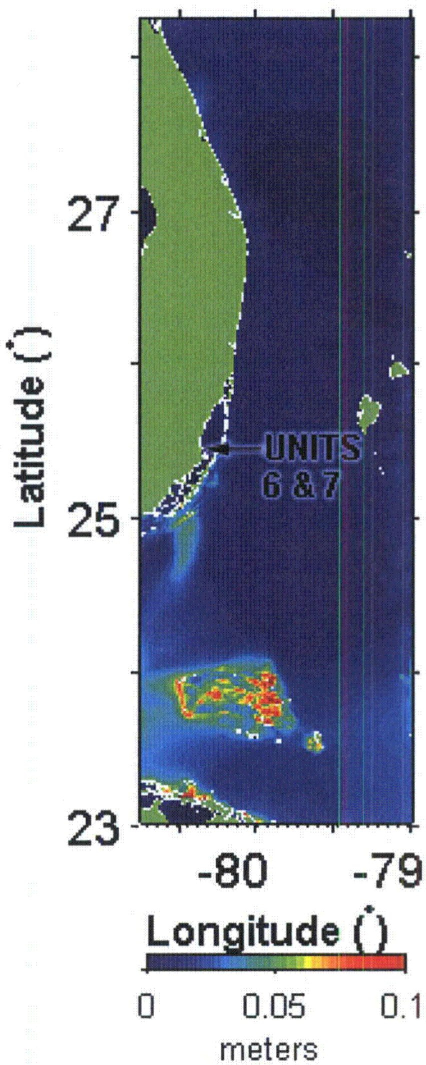

Figure 27. Simulated propagation of the Florida Escarpment tsunami (static source) in Grid C at 140, 160, 180, and 200 minutes after the submarine failure. Colors in elevation legend represent water surface elevations relative to MLW in meters.

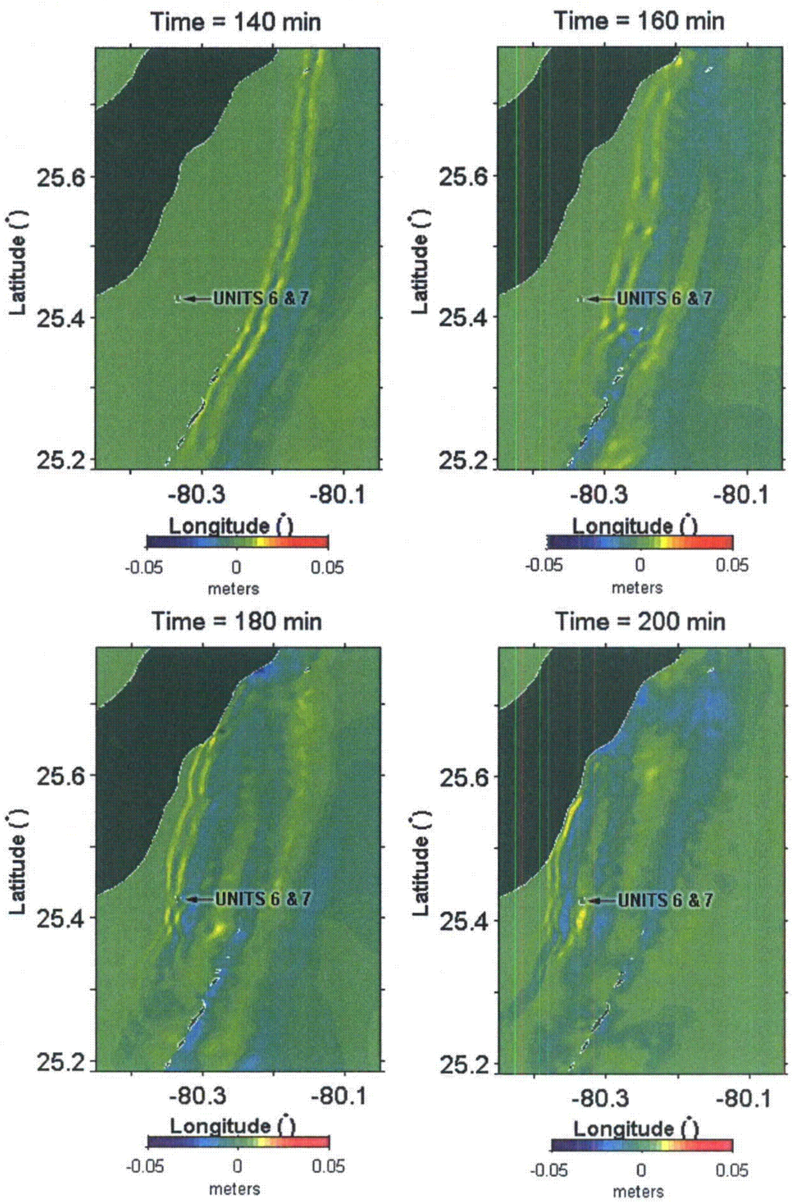

Figure 28. Simulated propagation of the Florida Escarpment tsunami (static source) in Grid C at 220, and 240 minutes after the submarine failure. Colors in elevation legend represent water surface elevations relative to MLW in meters.

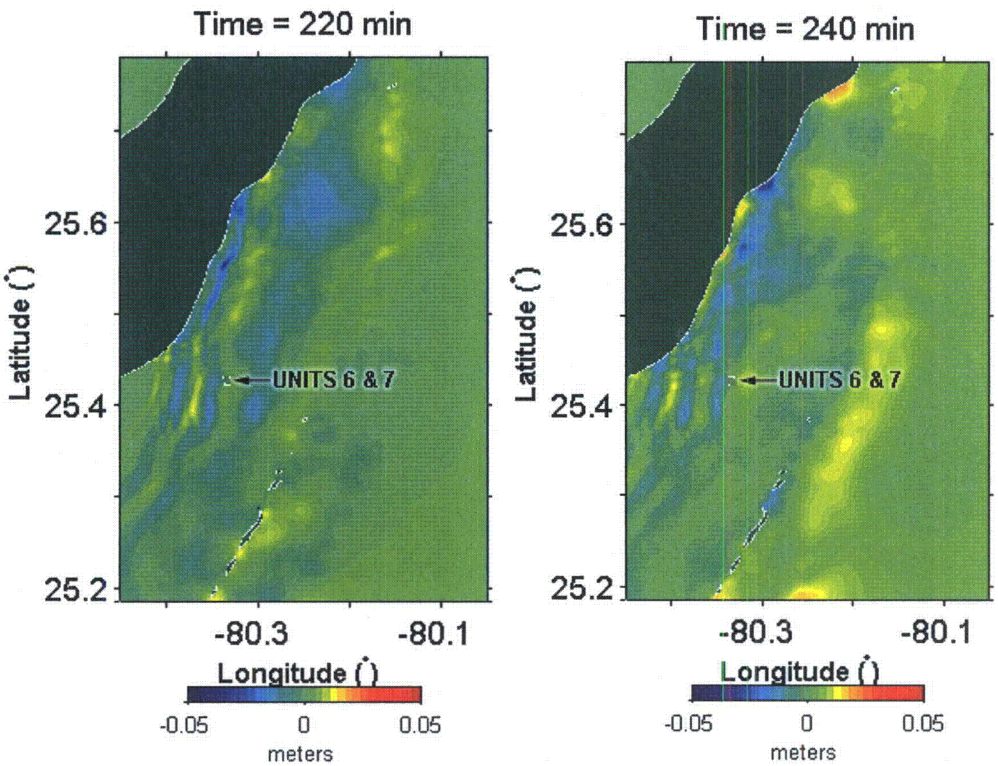

Figure 29. Simulated maximum water surface elevation during the propagation of the Florida Escarpment tsunami (static source) in Grid C. Colors in elevation legend represent water surface elevations relative to MLW in meters.

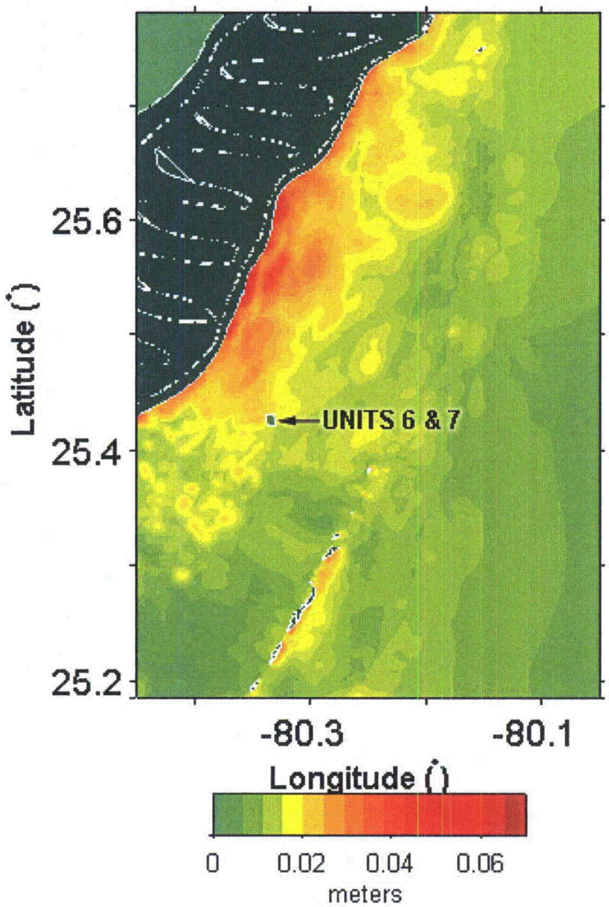

Figure 30. Simulated maximum water surface rise, relative to the initial sea water level, during the propagation of the Florida Escarpment tsunami (static source) in the vicinity of Units 6 & 7. Colors in elevation legend represent water surface elevations relative to MLW in meters.

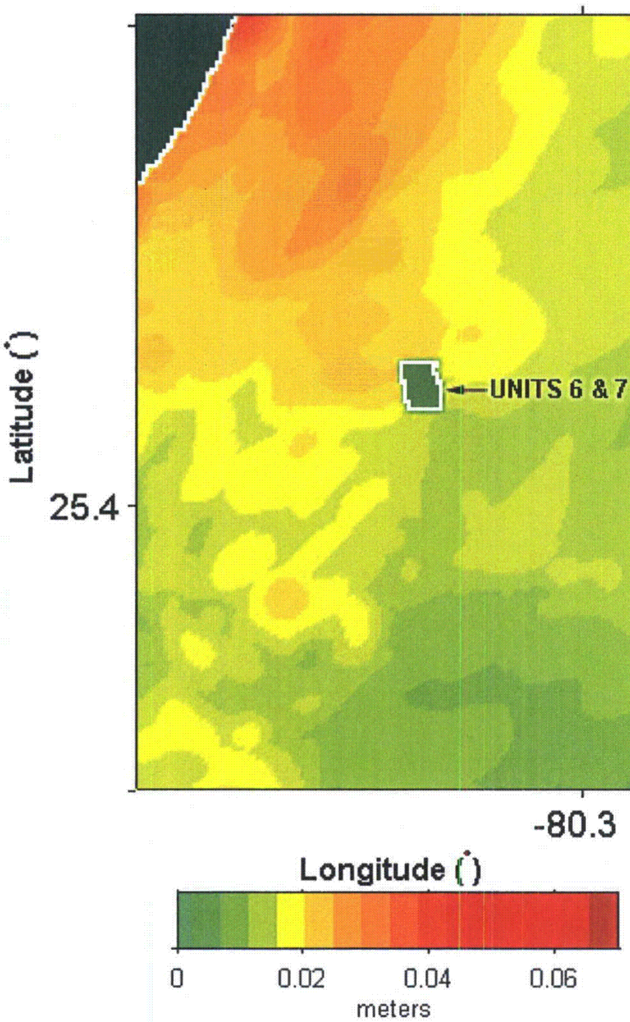

Figure 31. Water surface elevation at the FPL Turkey Point Units 6 & 7 as a function of time following the Florida Escarpment tsunami (static source). Water surface elevations are relative to the initial water level.

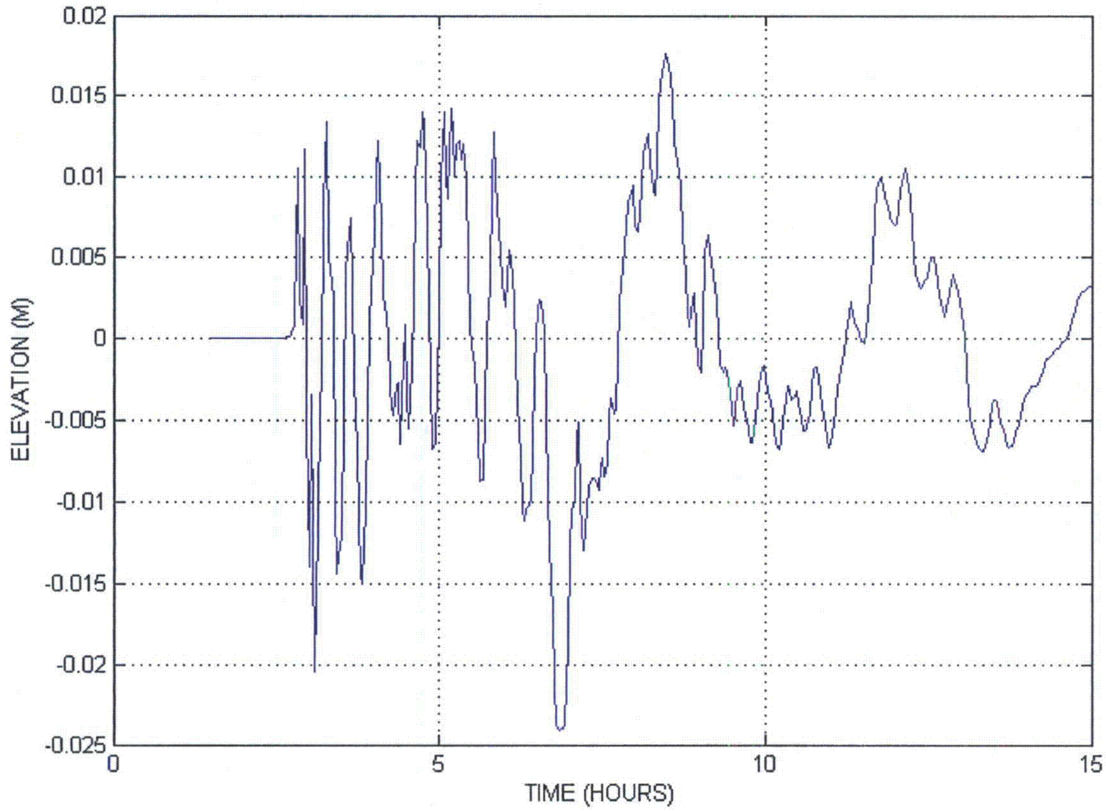

Part B – Evaluation of the Tsunamis from Submarine Slope Failures in the Great Bahama Bank

Sedimentary and Geomorphic Processes on and Affecting the Great Bahama Bank

A number of publications examined the various aspects of sediment deposits and sedimentary/geomorphic processes on and affecting the Great Bahama Bank (GBB), its western margin and the Straits of Florida. A review of the literature indicates that different investigators (References 25, 26, 27, 28, 29, 30, and 31) have proposed multiple hypotheses to explain the distribution of the cyclical successions of deposits as displayed in boring data obtained in the region (such as Ocean Drilling Program (ODP) Site 626, Clino borehole, and the Great Isaac Well, etc.) and interpreted from seismic reflection survey data as described below.

Mullins and Neumann (Reference 27) studied the carbonate deposits in the Bahamas using high-frequency; high resolution seismic reflection profiles and bottom grab samples. They determine that in general, the leeward deep bank margins are steeper, narrower, more dissected, and contain significantly greater amounts of coarse grained sediments than their windward margin counterparts. According to Mullins and Neumann (Reference 27), the processes that are responsible for the development of deep carbonate bank margins include: basement faulting, direction and magnitude of off bank sediment transport, oceanic circulation, gravity and pelagic sedimentation, submarine cementation and biological buildups. "Of these, basement faulting is primarily responsible for the initiation of carbonate platform edges. Off bank sediment transport is controlled by the physical energy flux such as winds, waves, storms at the sea surface and controls the availability of shallow water sediment for transport to the deep flanks" (Reference 27, p. 165).

Fulthorpe and Melillo (Reference 25) interpret the carbonate sediment cored at ODP Site 626 in the Straits of Florida to have been deposited by gravity flows having the characteristics of debris flows and high-density turbidity currents. These gravity flows could have been caused by gravitational instability that was the result of sediment loading of a carbonate platform slope during a period of rising sea level; triggering of slope failure by a decrease in sea level; or triggering by tectonics and earthquake activity during the middle Miocene.

Kuhn and Meischner (Reference 28) interpret the carbonate sediment from ODP Leg 101 Sites 628 (Little Bahama Bank), 632 (Exuma Sound), and 635 (Northeast Providence Channel) to have been deposited downslope during the initial stage of falling sea level. Gravity flows may have occurred along the entire slope, flowing downslope in a regional canyon system that was less prominent than on a steeper slope. Therefore, the gravity flows eroded and entrained large amounts of fine-grained slope sediment (Reference 28).

By examining the seismic data and limited well data from the northwestern GBB, Eberli et al. (Reference 29) interpret that the deposits developed as a result of pulses of prograding sediments generated by fluctuations in sea level and that an aggradation phase on the marginal slope preceded progradation. The timing, amount, and mode of progradation and the geometries of the prograding units are controlled by several factors such as sea level, subsidence, carbonate production and accumulation, direction of wave energy, and angle of repose. Eberli et al. (Reference 29, p. 1002) state that the "sea level changes are responsible for the pulsed mode of progradation, and the sequences seen on seismic lines."

Betzler et al. (Reference 30) interpret deposits of the Miocene-Lower Pliocene Bahamian carbonate ramp from core, geophysical logging, and high-resolution seismic reflection data from ODP Leg 166 (in the western margin of the GBB south of ODP Site 626 in the Straits of Florida). The deposits consist of cyclic alternations of light and dark grey wackestones/packstones with interbedded calciturbidite packages and minor slumps. These deposits are interpreted by Reference 30 to be the result of high-frequency sea level changes. Betzler et al. (Reference 30) propose two models to explain the cycle generation. The first model applies the principle of highstand shedding and correlates the dark-grey layers to low sea level (i.e., lowstands). The second model assumes that the dark-grey layers formed as condensed sections during sea level rises (i.e., highstands). Betzler et al. (Reference 30, pp. 1141-1142) favor the second model "because the shallow water carbonate production area was not reduced significantly during sea level lowstands...the dark-grey/light-grey cyclicity is linked to the Miocene ramp geometry...it disappeared during the Early Pliocene, as the ramp began to change into a flat-topped platform." In addition to high frequency sea level changes, Betzler et al. (Reference 30) interpret the depocenter shifts of Miocene gravity flows from an outer ramp position during the Early and Middle Miocene to a basin floor position during the Late Miocene and Early Pliocene (i.e., depocenter shifted from east to west) to be the result of increasing strength of bottom currents during the Late Miocene.

Betzler et al. (Reference 31) studied the shedding pattern along the slope and toe of slope deposits of the carbonate ramp of the western margin of the GBB using seismic lines, logging data, and quantitative petrographic data from ODP Leg 166. Betzler et al. (Reference 31) interpret two types of turbidite sequences; the first sequence is characterized by aggradation to weak progradation of the inner ramp which leads to gradual uphole increases in shallow water components within individual depositional sequences whereas, the second type formed during sea level falls and are characterized as fan depositional systems, which are laterally discontinuous. The first type of turbidite sequence on a large to medium seismic stratigraphy scale is laterally continuous over longer distances. The second type of turbidite sequence is characterized by a mixture of shallow water particles and other components with each turbidite package consisting of a distinct composition with no large scale compositional trends (Reference 31). Betzler et al. (Reference 31) interpret the shedding pattern to have recorded five orders of sea level changes with the turbidite packages reflecting the Middle Miocene sea level fall.

Considering the uncertainty in the actual mechanism of deposition of the sediments encountered at ODP Sites near the GBB, and evidences of sea bed instabilities as cited by some investigators, primarily evidence from recent high-resolution seismic reflection and bathymetry data (Reference 22), the potential of submarine slope failures along the western margin of the GBB and the associated tsunami flooding hazard at the Turkey Point Units 6 & 7 site warrants further evaluation.

Areas of Potential Submarine Slides along the Great Bahama Bank

Several areas that exhibit mass gravity flow deposits (Reference 32) occur on the western margin of the GBB. The western margin, which contains several areas of past and potential future slope failures have been studied by References 22, 24, 28, 34, and 35 for various purposes. The data provided by References 32, 34, and 35 comprise part of the Ocean Drilling Program (ODP) Legs 101 and 166 scientific investigations and proceedings. Paleontological, biostratigraphic, geochemical, geophysical (seismic reflection survey), and sedimentological data were collected from ODP Legs 101 and 166. Data documented in Reference 24 consists of high-resolution seismic reflection profiles with submersible reconnaissance and bottom sediment samples. More recently, Mulder et al. (Reference 22) (supported by the French Institut National des Sciences de l' Univers program "Action Marges") acquired new high-quality multibeam bathymetry, high-resolution seismic profiles, and seventeen gravity cores. The seismic reflection profiles (i.e., ODP Legs 101 and 166, and Reference 24) and multibeam bathymetry (i.e., Reference 22) contain features interpreted as the result of slope failure and mass gravity flow deposits (Figure 33). The seismic profiles (Figures 2 and 3 of Reference 24) are defined by a bank edge, a steep upper rocky slope interval or wall and a lower slope. FPL interprets the slopes observed on the seismic profiles to be relatively young; possibly Holocene in age. The data supporting this evaluation is comprised of the clean, sharp slope profiles in Figures 2 and 3 of Reference 24. In addition, the bathymetric images on Figure 1 of Reference 22, Figure 1 of Reference 21, and Figure 8 of Reference 23 depict what appear to be relatively steep slopes that do not indicate significant modification. In addition, Uranium/Thorium dating methods give dates of approximately 810 to 10,120 years before the present on cored sediments from the slope (Reference 24). These data support a Holocene age for the slope failures. While these deposits may have formed as a result of downslope (east to west) transport of sediment formed on the Bahama's bank top, Mulder et al. (Reference 22, p. 605) interpret the mass gravity flow deposits as a result of slope failures and state, "due to their large size, mass transport complexes can be tsunamigenic and have to be considered in the assessment of natural hazards." Therefore, it is conservatively assumed that a future failure in the slope instability areas on the western margin of the GBB can generate a tsunami. The two areas on the western margin of the GBB that are interpreted to have a potential to generate a probable maximum tsunami (PMT) to the Turkey Point Units 6 & 7 site are referred to as the southern site and the northern site as described below.

Southern Site

High-resolution multi-beam bathymetric and seismic reflection data collected recently have provided the basis for understanding the morphology of the western margin of the GBB and the adjacent sea floor of the Straits of Florida (References 21 and 22). These data display evidence of slope instabilities starting at a water depth of approximately 450 to 550 meters. Scars from slope failures are typically about one kilometer wide. These scars "evolve longitudinally toward a fan-lobe system in which erosional processes dominate over depositional systems. Tongue-shape patches of blind echo-facies are observed locally and could result from debris flow transport of reworked coarse sediment originating from the bank, or from deep-water coral mounds. The most impressive morphological feature is a large sediment failure and its associated mass transport complex" (Reference 22) (Figure 34). This mass gravity flow feature includes three failure scarps, spanning an area about 9 kilometers wide and ranging in height from 80 to 110 meters. Downslope of the scars, the seafloor is hummocky in nature (i.e., debris field). The debris field extends westward over 20 kilometers. The surface of the entire deformed area is approximately 300 square kilometers (Reference 22). This area, referred to as the southern site as shown in Figure 34, is located at approximately 24.9534° N, 79.2358° W and is approximately 90 kilometers west of the Great Bahama Island, about 90 kilometers south of the Bimini Islands and 125 kilometers from the Turkey Point Units 6 & 7 site. Figure 35 shows a profile of the bathymetry at this location. As shown in Figure 35, the length of the steeper slope (>1.5 degrees) along this profile is approximately 3 kilometers with the upper part of the profile having a slope of about 5.8 degrees, while the middle part of the profile has a slope of about 3.8 degrees. Figure 32, which is reproduced from Figure 1D of Reference 22, shows these scars and suggests that a larger area that encompasses these scars and some smaller adjacent scars is about 14 to 15 kilometers wide which is consistent with the 13 kilometers width stated in Mulder et al. (Reference 22). The large- and small-scale morphologies in this area "include bypass areas, channel-levee lobe systems, gullied slopes, and products of slope instabilities at various scales, including long slump scars at the lower slope and mass transport complexes that extend approximately 30 kilometers into the adjacent basin floor" (Reference 22).

Northern Site

The northern site is located at approximately 25.6134° N, 79.3213° W, approximately 104 kilometers east of the Turkey Point Units 6 & 7 site, as shown in Figure 34. This location is the closest potential slope failure area to the Turkey Point Units 6 & 7 site. This area is discussed in detail in Reference 24 and is briefly summarized here. It is described as consisting of a bank edge, a lithified accretionary slope (steep rocky slope interval or wall and thinned Holocene sequence), and a lower slope. The bank edge consists of vertical (1-5 meters) steps, separated by gently sloping, sediment covered terraces in water depths of less than 10 meters. The lower part of this interval is smooth or hummocky with a surface of thin (10-30 centimeters) hardgrounds (i.e., cementation by either aragonite or Mg-calcite) (References 24 and 33). A monotonous and generally smooth lithified accretionary slope with a gradient of approximately 15 to 20 degrees is located west and downslope of the bank edge. The water depth at its upper, shallow end occurs at depths between 15 and 65 meters. The deeper part of the slope occurs in water depths of 65 to 150 meters. The 1-5 meter wide ledges in the upper portion of the slope appear to act as steps for cascading sand from above. However, near Bimini and Riding Rocks, the accretionary slope is described as a vertical wall (>45 degrees) that is locally undercut between 35 and 80 meters. Below this wall, the slope gradients decrease from 30 to 35 degrees at 100 meters to 15 degrees at 300 meters. The slope is concave and lithified throughout the lower interval (References 24 and 33). Seaward of this location, a trough and "dump bump" topography marks the beginning of the lower slope. The lower slope west of and below the "dump bump" is a very low energy environment, found in water depths greater than 150 meters.

Figure 38 shows the bathymetry of the northern site near the Bimini Islands which exhibits failure scars, "Fs" (Reference 22). Figure 36 shows the location of several seismic reflection profiles presented in Reference 24. The seismic reflection profile along Line 5 in the study area near Bimini Island, which is the closest in distance to the potential slope failure area postulated for the Turkey Point Units 6 & 7 site, is shown in Figure 37. Near the top of the profile of Line 5, the steepest slope is about 20 degrees. Within about 1 kilometer, the slope decreases to approximately 17 degrees and further west (downslope) to 5 degrees along the profile. In comparison, the slope of the face of the scarp at the northern site, based on the bathymetry profile shown in Figure 39, is about 7 degrees. Different seismic profiles presented in Reference 24 suggest that low angle slopes to 20 degrees slope could be subject to failure.

Therefore, among slope failures of similar size, the impact on the Turkey Point Units 6 & 7 site would depend on the proximity of the tsunami source, the direction of the wave, and the bathymetry along the path of its propagation. The northern site location is referred to henceforth as the Postulated Slide Location. Based on this consideration, the Postulated Slide Location shown in Figure 34 and Figure 36 was identified as being the most likely in the GBB to generate a tsunami that would produce the maximum wave height at the Turkey Point Units 6 & 7 site. The Postulated Slide Location is about 13 kilometers southwest of South Bimini Island. At a distance of about 104 kilometers, the Postulated Slide Location at this point along the western margin of the GBB is the closest to the Turkey Point Units 6 & 7 site with the direction of a potential failure pointing directly towards the site.

The conservative approach to the GBB tsunami flooding evaluation is to incorporate source characteristics from both of the hypothetical slide areas described above. The northern site, at approximately 25.6134° N, 79.3213° W, is therefore selected as the source location of the postulated slide for the tsunami modeling because of its proximity and direct path of tsunami wave propagation to the Turkey Point Units 6 & 7 site.

Representation of the GBB Slide in the Model Simulations

The maximum credible slide was schematized for modeling purposes as having a Gaussian shape with an elliptical footing. This shape was chosen because a Gaussian shape has been used for several investigations and studies of landslide tsunamis, including benchmark cases (References 9, 14, 18). Grilli and Watts (Reference 9) state that a Gaussian shape is a more realistic representation of a submarine mass failure than other arbitrary fixed shapes. Enet & Grilli (Reference 8) used a Gaussian shape in the experiments that provide the basis for the validation of the model used to simulate the generation of a wave by a submarine slide (Reference 8). Although actual slides usually have more pronounced head shapes, the Gaussian surface shape is deemed as providing a reasonable approximation of the shape of actual slides. The Gaussian shape of the slide was approximated in the numerical model by truncated hyperbolic secant squared functions. The center of the elliptical base of the slide prior to the initiation of movement is located at 25.6134° N, 79.3213° W. The length (minor axis of the elliptical base) of the slide is 3 kilometers, and its width (major axis of its elliptical base) of the slide is approximately 30 kilometers.

The length of the slide is postulated based on the ocean floor profile at the site investigated in detail by Mulder et al. (Reference 22) shown in Figure 35, where the length of the steepest slope in the southern site with a slope up from approximately 1.5 degrees is about 3 kilometers. Figure 37 shows that the length of the steepest slope at the Postulated Slide Location of the northern site with slopes greater than 5 degrees is close to 1 kilometer. As a conservative assumption, the larger failure length between the northern and southern sites, i.e., 3 kilometers, is selected to define the source (Case 1) in the numerical simulations.

The width of the slide, i.e., its dimension in the direction normal to the direction of the slope failure, is conservatively selected to be 30 kilometers. This width is about twice the combined width of all the scars identified in the southern site through multi beam bathymetric surveys shown in Figure 32.

The height of the three scars in the southern site shown in Figure 32 is between 80 and 110 meters (Reference 22). The upper end of this range is selected as a conservative estimate of the slide thickness at both postulated tsunami source locations along the GBB. It is also noted that the thickness of the material subject to potential mass failure on the seismic profile shown in Figure 37 (Line 5 in Reference 24) near the northern site is of the order of 100 meters.

The slope of the face of the scarp of the southern site shown in Figure 32 ranges from 3.8 to 5.8 degrees as illustrated in Figure 35. The slope of the ocean floor beyond the foot of the scarp is of the order of 1.5 degrees. The slope of the face of the scarp at the Postulated Slide Location in the northern site, based on the profile shown in Figure 39, is about 7 degrees. This slope is used in the simulation of a 3-kilometer long slide, presented as Case 1. The center of the elliptical base of the Case 1 slide was placed at 25.59° N, 79.33° W. In addition, the effect of a steeper but shorter potential slide is evaluated in Case 2. Based on the seismic profile shown in Figure 37, reproduced from Reference 24, the source in Case 2 is represented by a bed slope of 20 degrees and a slide length of 1.5 kilometers. The center of the elliptical base of the Case 2 slide was placed at 25.62° N, 79.34° W.

For Case 1, the initial acceleration of the 3-kilometer slide on a 7-degree bed slope is 1.2 meters per second squared, and its terminal velocity 58.3 meters per second. This estimate was obtained using a specific gravity for the slide equal to 2, and global drag coefficient equal to 1. Based on its initial acceleration the slide reaches its terminal velocity within 49 seconds. For Case 2, the initial acceleration of the 1.5-kilometer slide on a 20-degree bed slope is 3.4 meters per second squared, and its terminal velocity 69.1 meters per second, reached in 21 seconds from the initiation of motion.

Initial Wave Generated by the GBB Slide

Two alternative approaches were used for the generation of the initial wave in the tsunami simulations. The two approaches are referred to as the dynamic source approach and the static source approach.

The dynamic source approach defines the initial condition for the tsunami propagation simulations in terms of both the water surface displacement and the depth-averaged horizontal velocity fields. This source was computed from the slide geometry and its movement using the computer model NHWAVE (Non-Hydrostatic Wave), Version 1.1 (Reference 10). NHWAVE solves the fully non-hydrostatic Navier-Stokes equations in the sigma coordinate system.

Input to NHWAVE includes the bathymetric grid, the slide dimensions, the initial slide position and orientation, the terminal velocity, and the down-slope acceleration of the slide. For the dynamic approach, the modeled domain was set up so that the landslide event was centrally located and the generated motion did not reach the lateral boundaries during the simulated time. Results from the NHWAVE model at the time the amplitude of the generated wave becomes equal to the maximum thickness of the slide were saved and used as initial conditions in the tsunami propagation model FUNWAVE-TVD.

The present approach conservatively neglects the spreading and flattening of the sliding mass during the slide process in the present simulations. This results in a higher and narrower initial elevation hump at the final slide location than what would have occurred if the slide were allowed to deform. The initial and final positions of the 3-kilometer slide are displayed in Figure 41.

For Case 1 that simulated the 3-kilometer slide on a 7-degree slope, the NHWAVE model was run for a period of time and the surface displacement field and horizontal velocity fields at 110 seconds, the time that the maximum drawdown (negative wave height) became about equal to the maximum thickness of the slide were saved and used as input into FUNWAVE-TVD. The resulting water surface displacement from NHWAVE at that time

(110 seconds) for the 3-kilometer slide on a 7-degree slope is shown in Figure 42 and Figure 43, which also shows the evolution of the simulated water surface profile over time in the direction of the slide motion simulated with NHWAVE after the initiation of the slide. The maximum water surface at 110 seconds is 63 meters, and the minimum –108 meters.

For Case 2 that simulated the 1.5-kilometer slide on a 20-degree slope, the NHWAVE model was run until the maximum drawdown became about equal to the maximum thickness of the slide, which in this case was 140 seconds. Figure 51 shows the water surface at that time which was used as input in the FUNWAVE-TVD simulation. The maximum water surface is 61 meters and the minimum -120 meters. Figure 52 shows the evolution of the simulated water surface profile over time.

The second approach to the generation of the initial condition for the tsunami propagation model used a static source. A static source is defined as an initial displacement of the water surface in the form of a depression over the initial slide location, equal in areal extent, shape and volume to the displaced material volume during the submarine slide. A negative displacement of the water surface equal to the volume, shape and areal extent of the slide was assumed at the initial slide location, i.e., extending over an elliptical area with minor axis equal to 3 kilometers, major axis 30 kilometers and maximum thickness 110 meters. A corresponding positive displacement representing the missing volume of the slide mass was also added. The centroid of the depression of the water surface was placed at 25.63° N, 79.34° W.

The source parameters and initial wave characteristics for the three model cases are summarized in Table 2.

Modeling of Tsunami Propagation and Inundation

The propagation, shoreline runup and inundation caused by the GBB slide were simulated using the Boussinesq wave model FUNWAVE-TVD, developed at the University of Delaware. In its present application, FUNWAVE-TVD solved the spherical-polar form of the weakly-nonlinear, weakly-dispersive Boussinesq equations described in Reference 11. Reference 12 describes both the Cartesian and the spherical-polar versions of the code. The model incorporates bottom friction and subgrid lateral turbulent mixing effects.

The Cartesian coordinate version of FUNWAVE-TVD, described in References 12 and 13 has been validated using several PMEL-135 benchmarks (Reference 14), which are the presently accepted benchmarking standards adopted by the National Tsunami Hazard Mitigation Program (NTHMP) for judging model acceptance for use in development of coastal inundation maps and evacuation plans. Benchmark tests for the Cartesian version of FUNWAVE-TVD are described in Reference 12. Benchmark tests for the spherical version of the code are described in Reference 11.

The equations solved by FUNWAVE-TVD consist of a depth-integrated volume conservation equation together with depth-integrated horizontal momentum equations. These equations are summarized in References 12 and 13. For tsunami applications, FUNWAVE-TVD is run with closed boundaries and an initial hot start condition consisting of either a surface displacement alone (in the case of static initial conditions) or a surface displacement and initial velocity field (in the case of a dynamic initial condition based on the simulation results of NHWAVE). The model is run from the initial start until past the time when significant wave activity has decayed at the target site.

In most large scale problems, FUNWAVE-TVD is run on more than one nested grid. The grid nesting scheme uses a one-way nesting technique, which passes surface elevation and velocity components calculated from a large domain to a nested small domain through ghost cells at nesting boundaries. A linear interpolation is performed between the large and the small domain at the nesting boundaries. A test of the nesting process is included in the FUNWAVE-TVD verification and validation document (Reference 12).

In the simulations of the tsunami generated by a landslide on the western margin of the GBB, two grids are used, which are referred to as Grid B and Grid C. These are the same grids used in analysis of tsunamis generated by a submarine slide at the Florida Escarpment described in Part A of this response. The output from Grid B is used as input to FUNWAVE-TVD on Grid C.

The domain covered by each of the grids is shown in Figure 40. All the grids are based on geographic coordinates. The coordinates of the southwest corner of each grid, the grid size and number of grid cells in each grid are given in Table 1.

Table 1. Nested grids used in FUNWAVE-TVD for Great Bahama Bank Tsunami

Grid	Coordinates of SW Corner		Grid Spacing	Number of Grid Cells
	X	y	$\Delta x = \Delta y$	
	degrees	degrees	seconds	cells
B	-80.75	23.0	15	480 x 1260
C	-80.517	25.156	3	592 x 768

It is noted that because of the curvature of the earth, having a uniform grid size in degrees leads to variable-length (in the west-east direction) cells at different latitudes within the model domain.

There is a sponge layer along the open boundaries of the model which was used for the definition of the boundary conditions. The thickness of the sponge layer was 40 kilometers along the eastern and the western boundary, 50 kilometers along the southern boundary and 20 kilometers along the northern boundary.

The antecedent water surface level used for the model simulation was equal to the 10 percent exceedance high tide level, plus the initial rise and long term sea level rise, which produce an initial water level equal to 1.68 meters (5.5 feet) mean low water (MLW), or 3.6 feet (1.10 meters) NAVD 88, same as that used for the PMT numerical simulation in FSAR 2.4.6.4 and for the probable maximum storm surge evaluation as explained in FSAR 2.4.5.2.2.1.

Simulation Results

Simulations were performed for three cases representing different assumptions for the initial tsunami wave that can be generated by a submarine slide at the west margin of the GBB. Case 1 uses a dynamic source, i.e., a wave produced by NHWAVE, for a tsunami generated by a 3-kilometer slide on a 7-degree slope. Case 2 uses also a dynamic source for a tsunami generated by a 1.5-kilometer slide on a 20-degree slope. Case 3 uses a static source for a tsunami generated by a 3-kilometer slide on a 7-degree slope.

With respect to Case 1, Figure 44 shows the propagation of the tsunami wave in Grid B, at 2, 4, 6 and 14 minutes in the FUNWAVE-TVD simulation. Figure 45 shows the maximum water surface elevation within the model domain of Grid B during the simulation period.

Figure 46 shows the propagation of the same tsunami wave in Grid C, at 18, 30, 44 and 100 minutes in the FUNWAVE-TVD simulation. Figure 47 shows the maximum water level over Grid C. As can be seen in these figures the area surrounding Turkey Point Units 6 & 7 site is inundated. The Units 6 & 7 site itself and other parts of the Turkey Point station, which are elevated above the existing grade, are not inundated and remain dry. The inundation of the area surrounding the site of Units 6 & 7 is not caused by the GBB tsunami. It is a consequence of the assumption regarding the initial sea water level that accounts for the 10 percent exceedance high tide level of 3.6 feet mean low water (MLW), initial rise of 0.9 feet and long term sea level rise of 1.0 foot, the sum of which produces an initial water level, i.e., prior to the arrival of the tsunami, equal to 1.68 meters (5.5 feet) MLW, or 3.6 feet (1.10 meters) NAVD 88. This initial water level is enough to inundate a large zone along the Florida coast, including the area around Units 6 & 7. Again, the Units 6 & 7 site itself and other parts of the Turkey Point station, which are elevated above the existing grade, are not inundated and remain dry. The effect of this initial water level is made clear in Figure 48, which shows the water depth over the area of Grid C relative to two different levels of the water surface. Figure 48(a) shows the water depth relative to MLW without the water level rise that is used to define the initial condition for the tsunami propagation simulations. Figure 48(b) shows the water depth relative to the assumed initial water surface in the west margin GBB tsunami simulations, i.e., relative to 10 percent exceedance spring tide + initial rise + long-term sea level rise. Figure 49 shows the maximum water surface rise in the vicinity of the site, relative to the initial sea water level.

Figure 50 shows the water level at the Turkey Point Units 6 & 7 site as a function of time. The maximum water surface level rise over the initial water level is 2.9 meters, occurring about 50 minutes from the initiation of the slide. The predicted maximum water surface level is 4.6 meters (15.0 feet) MLW, or 4.0 meters (13.1 feet) NAVD 88. The predicted maximum water level near the site is derived from Figure 49.

With respect to Case 2, Figure 51 shows the water surface profile simulated with NHWAVE that was used as input in the simulation of the propagation of a tsunami caused by a 1.5 kilometers long slope failure on a 20-degree slope.

The simulation with FUNWAVE-TVD was again performed in two steps, modeling the propagation of the tsunami wave first within Grid B, then in Grid C using the output from the Grid B as input in Grid C to define the wave surface elevation and velocity conditions along its boundaries. Figure 53 shows the propagation of the tsunami wave in Grid B, at 2, 6, 8 and 14 minutes in the FUNWAVE-TVD simulation.

Figure 54 shows the maximum water surface elevation within the model domain of Grid B during the simulation period. Figure 55 shows the propagation of the same tsunami wave in Grid C, at 18, 30, 44 and 100 minutes in the FUNWAVE-TVD simulation. Figure 56 shows the maximum water level over Grid C. As in Case 1, the area surrounding Turkey Point Units 6 & 7 site is inundated but the Units 6 & 7 site itself and other parts of the Turkey Point station, which are elevated above the existing grade, are not inundated and remain dry. The inundation of the area surrounding the site of Units 6 & 7 is not caused by the GBB tsunami. It is a consequence of the assumption regarding the initial sea water level that accounts for the 10 percent exceedance high tide level of 3.6 feet mean low water (MLW), initial rise of 0.9 feet and long term sea level rise of 1.0 foot, the sum of which produces an initial water level, i.e., prior to the arrival of the tsunami, equal to 1.68 meters (5.5 feet) MLW, or 3.6 feet (1.10 meters) NAVD 88. This initial water level is enough to inundate a large zone along the Florida coast, including the area around the Turkey Point Units 6 & 7 site, as illustrated in Figure 48. Again, the Units 6 & 7 site itself and other parts of the Turkey Point station, which are elevated above the existing grade, are not inundated and remain dry. Figure 57 shows the maximum water surface rise in the vicinity of the Turkey Point Units 6 & 7 site, relative to the initial sea water level.

Figure 58 shows the time history of the water level at the Turkey Point Units 6 & 7 site. The maximum water surface level caused by this tsunami is 3.0 meters over the initial water level, also occurring after about 50 minutes from the initiation of the slide. The predicted maximum water surface level is 4.68 meters (15.4 feet) MLW, or 4.1 meters (13.5 feet) NAVD 88, taking into account the antecedent sea water level. The predicted maximum water level near the site is derived from Figure 57.

With respect to Case 3, the initial displacement of the water surface in this case is in the form of a depression approximately equal to the slide, i.e., extending over an elliptical area with its minor axis equal to 3 kilometers, its major axis equal to 30 kilometers and maximum thickness 110 meters. The volume of the depression is about 3 cubic kilometers. A water rise equal to the depression, both in shape and size, is formed downslope of the initial depression. The displacement volume of the positive wave and negative wave were set equal to the landslide volume. The maximum water surface rise is equal to 110 meters, equal to the height (thickness) of the slide. Figure 59 shows the assumed initial water surface wave for the tsunami simulation with FUNWAVE-TVD based on a static source.

Figure 60 shows the propagation of the tsunami wave in Grid B, at 2, 4, 6, and 14 minutes in the FUNWAVE-TVD simulation. Figure 61 shows the maximum water surface elevation within the model domain of Grid B during the simulation period. Figure 62 shows the propagation of the tsunami wave in Grid C, at 18, 30, 44, and 100 minutes in the FUNWAVE-TVD simulation. Figure 63 shows the maximum water level over Grid C.

Figure 64 shows the maximum water surface rise in the vicinity of the Turkey Point Units 6 & 7 site, relative to the initial sea water level. Figure 65 shows the water level at the site from the static source simulation as a function of time. The maximum water surface rise caused by the tsunami generated by a submarine slide at the Postulated Slide Location is 1.7 meters over the initial water level, occurring after about 58 minutes from the initiation of the slide. The predicted maximum water level at the Turkey Point Units 6 & 7 site is 3.38 meters (11.1 feet) MLW, or 2.8 meters (9.2 feet) NAVD 88, taking into account the antecedent sea water level. The predicted maximum water level near the site is derived from Figure 64.

Summary of Results

A literature review was performed to identify the location and characteristics of potential submarine slope failures along the western margin of the GBB. Conservative assumptions were made to define such a submarine slide as a source of a tsunami event. The characteristics of the potential slope failure used to define the initial wave in the tsunami simulations were selected based on review and interpretation of the multibeam bathymetric data, seismic profiles, and other investigations reported in the literature (References 21, 22, 23, and 24). The postulated location of such a slope failure was selected to produce a tsunami wave that would cause the highest water level rise at the Turkey Point Units 6 & 7 site. The center of this postulated submarine slide is at 25.6134° N, 79.3213° W, approximately 13 kilometers south of South Bimini Island and about 104 kilometers from the Turkey Point Units 6 & 7 site.

The maximum credible submarine slide along the western margin of the GBB was schematized as having a shape similar to that described in Reference 8, i.e., as having an elliptical base with its minor and major axes equal to the length and width of the slide area, 3 kilometers (in the direction of motion), respectively. The maximum thickness of the schematized slide was 110 meters.

Simulations with two alternative initial conditions for the wave at the onset of the tsunami event were made, first assuming dynamic conditions including an estimate of the water surface displacement and the associated velocities, and second assuming static conditions that consist of an assumption of the water displacement and zero initial velocities. In both cases the assumed initial sea water level includes the 10 percent exceedance spring tide, an initial rise plus the long-term sea level rise, all of which add up to 1.68 meters (5.5 feet) MLW or 1.10 meters (3.6 feet) NAVD 88. As explained above, this is independent of the effect of the tsunami from a slide at the west margin of the GBB.

The non-hydrostatic code NHWAVE was used to simulate the motion of the slide and simulate the water surface elevation and horizontal velocities used as initial conditions in the simulation of the tsunami propagation with the Boussinesq code FUNWAVE-TVD. Two different combinations of slide length and slope were analyzed for the dynamic source approach, a 3-kilometer long slide on a 7-degree slope, and 1.5-kilometer long slide on a 20-degree slope, referred to as Case 1 and Case 2, respectively. The terminal velocity for the Case 1 slide was 58.3 meters per second, and for the Case 2 slide it was 69.1 meters per second. The initial maximum wave and negative (depression) wave produced by NHWAVE for Case 1 were 63 meters and -108 meters, respectively. The initial maximum wave and negative wave for Case 2 were 61 meters and -120 meters, respectively. The propagation of the tsunami was simulated through two grids, Grid B and Grid C, the latter grid having a finer resolution than the former grid. The predicted maximum relative water surface level rise at Turkey Point Units 6 & 7 site for Case 1 is 2.9 meters above initial sea water level of 1.68 meters MLW, and the predicted maximum water level is 4.58 meters MLW or 4.0 meters NAVD 88. For Case 2, the predicted maximum relative water surface rise at the Turkey Point Units 6 & 7 site is 3.0 meters above initial sea water level of 1.68 meters MLW, and the predicted maximum water level is 4.68 meters MLW or 4.1 meters NAVD 88.

In addition a simulation was made for a static source, which is referred to as Case 3. The initial water surface displacement was assumed to be a dipole with a depression and a rise of water in the shape of the displaced mass of the submarine failure. In this approach, the initial water surface condition for the FUNWAVE-TVD simulations includes a 110-meters depression of the water surface over the slide and a 110-meters rise downslope of the slide. The initial velocity field in the static source approach is zero. For Case 3, the predicted maximum water level rise at the Turkey Point Units 6 & 7 site is 1.7 meters above initial sea water level of 1.68 meters MLW, and the predicted maximum water level is 3.38 meters MLW or 2.8 meters NAVD 88.

Table 2 summarizes the size of the initial wave and the predicted maximum water level at the Turkey Point Units 6 & 7 site for the three simulated cases.

Table 2. Summary of Simulated Cases for the Postulated GBB Slope Failures

Case	Description	Slide				Initial Wave		At Turkey Point Units 6 & 7 Site	
		Length	Width	Max Height	Bed Slope	Positive	Negative	Max Rise	Max Water El.
		kilometers	kilometers	meters	degrees	meters	meters	meters	meters (NAVD 88)
1	Dynamic source from NHWAVE	3	30	110	7	63	-108	2.9	4.0
2	Dynamic source from NHWAVE	1.5	30	110	20	61	-120	3.0	4.1
3	Static source	3	30	110	7	110	-110	1.7	2.8

Conclusions

Simulations were performed for a tsunami generated by a conservatively large slope failure along the western margin of the GBB. The maximum predicted water level at the Turkey Point Units 6 & 7 site due to this tsunami event is 4.68 meters (15.4 feet) MLW, or 4.1 meters (13.5 feet) NAVD 88. The assumed initial sea water level in the FUNWAVE-TVD model simulation includes the 10 percent exceedance spring tide, an initial rise plus the long-term sea level rise, all of which add up to 1.68 meters (5.50 feet) MLW or 1.10 meters (3.6 feet) NAVD 88.

The maximum predicted water level at the Turkey Point Units 6 & 7 site caused by a tsunami at the GBB is less than the maximum water level predicted for the 1755 Lisbon earthquake PMT scenario, which was estimated to be equal to 4.2 meters (13.9 feet) NAVD 88.

Figure 32 Three-dimensional View of Mass Transport Complex at the Great Bahama Bank

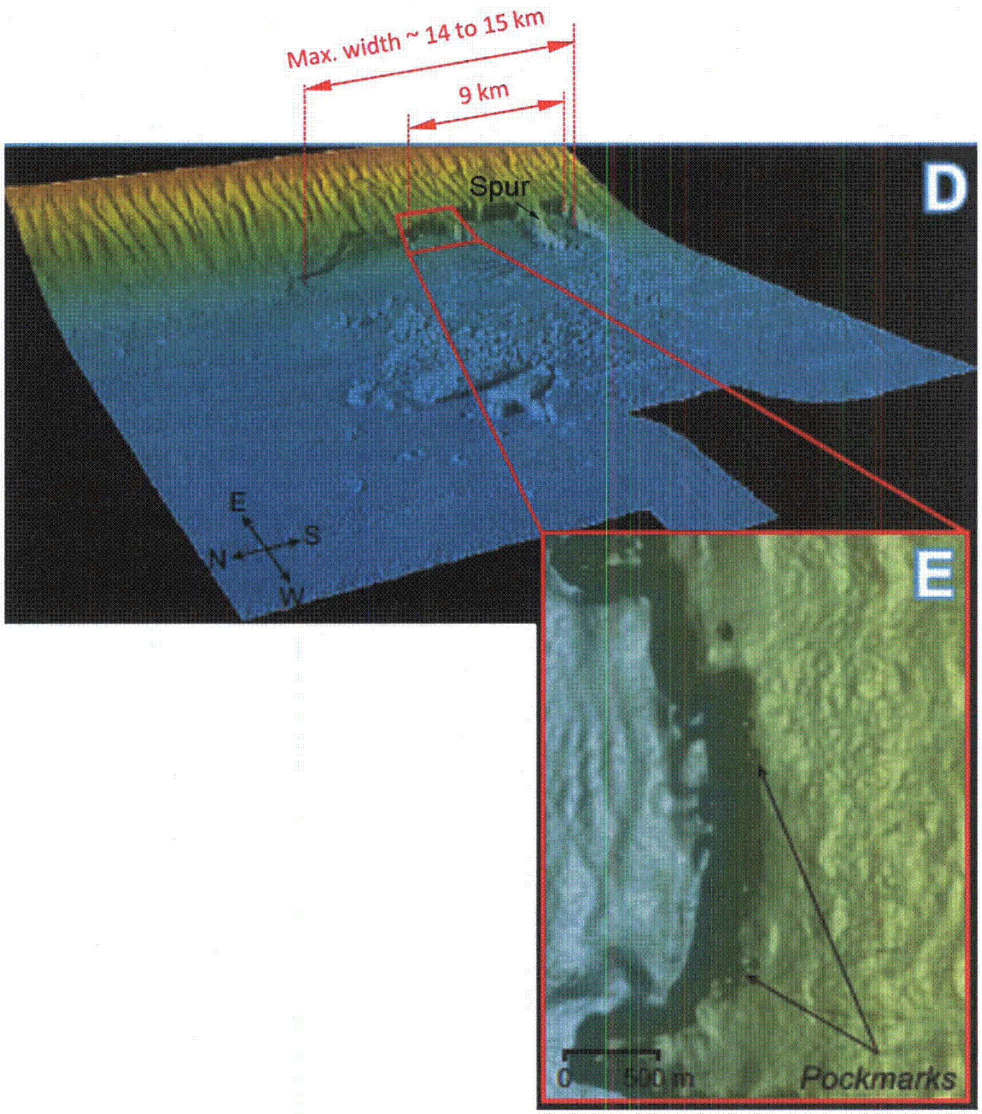

Source: Modified from Reference 22

Figure 33 (a) Three-dimensional View of the Two Southern Scars (b) Generalized Profile Showing the Variability of Mound Size with Respect to the Off-bank Sediment Deposits Across the GBB Slope; and (c) Schematic Three-dimensional Representation of the Slide

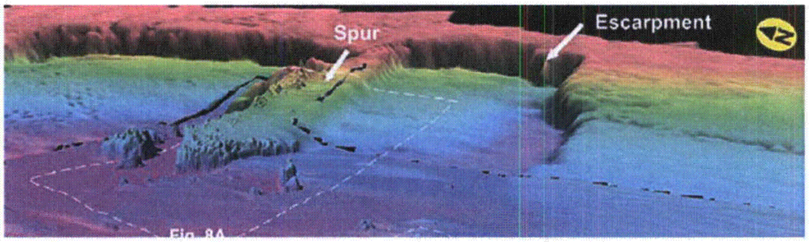

(a)

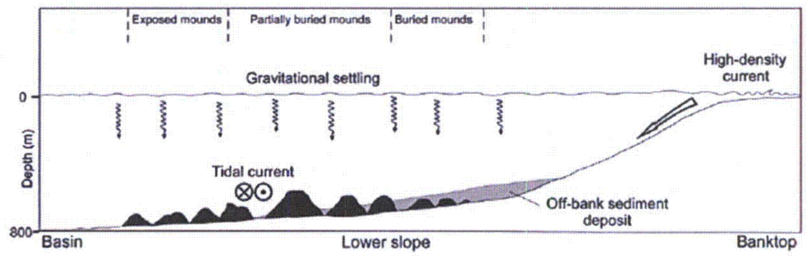

(b)

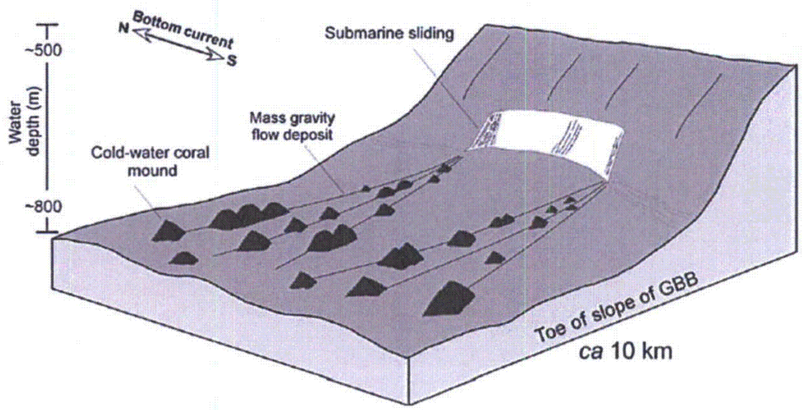

(c)

Source: Modified from Reference 36

Figure 34 Location of Postulated Submarine Slide Locations Along the Great Bahama Bank

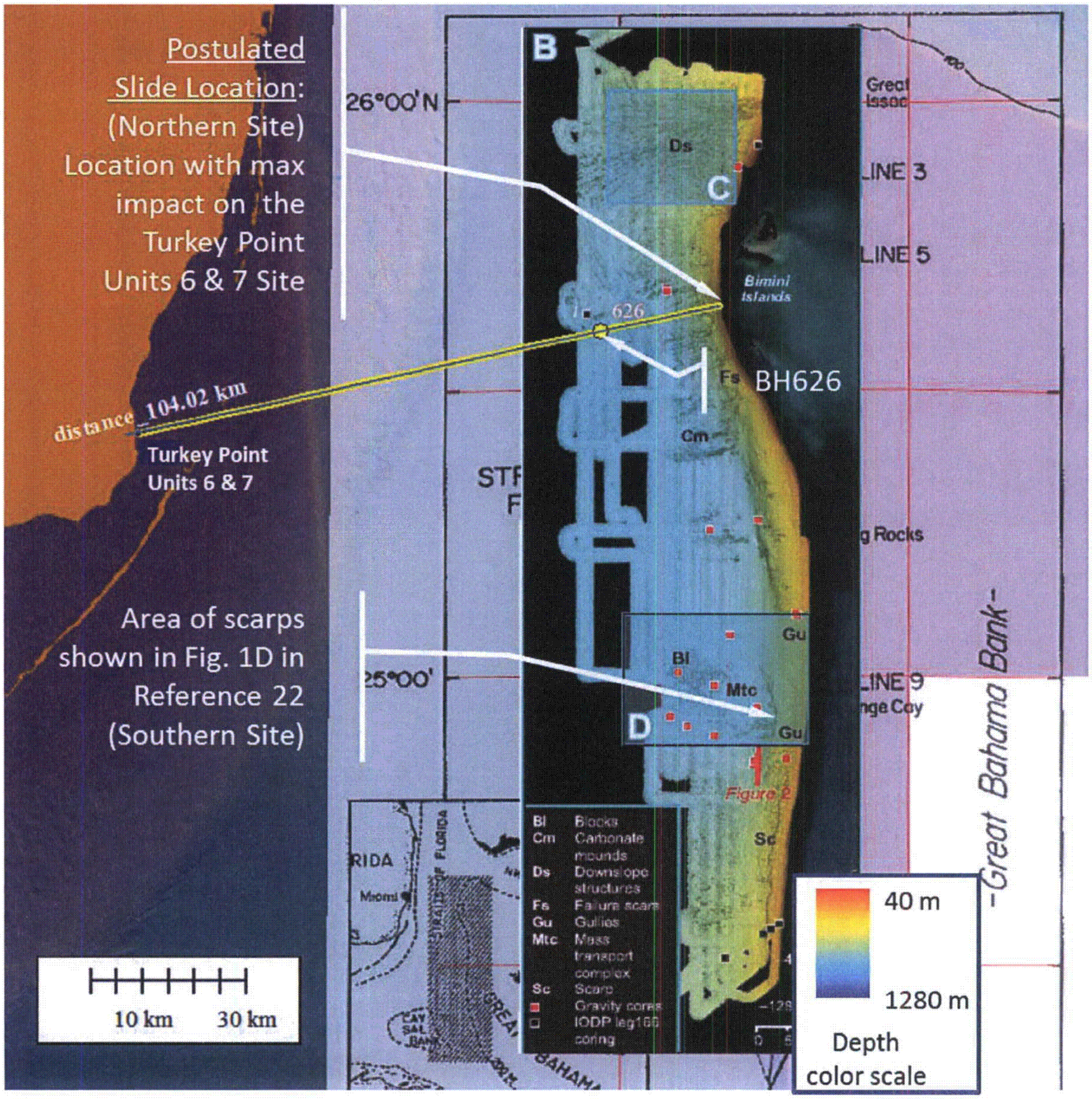

Source: Modified from Reference 22

Figure 35 (a) Ocean Bottom Profile Along Line A-A'; (b) Map Showing the Location of Line A-A'

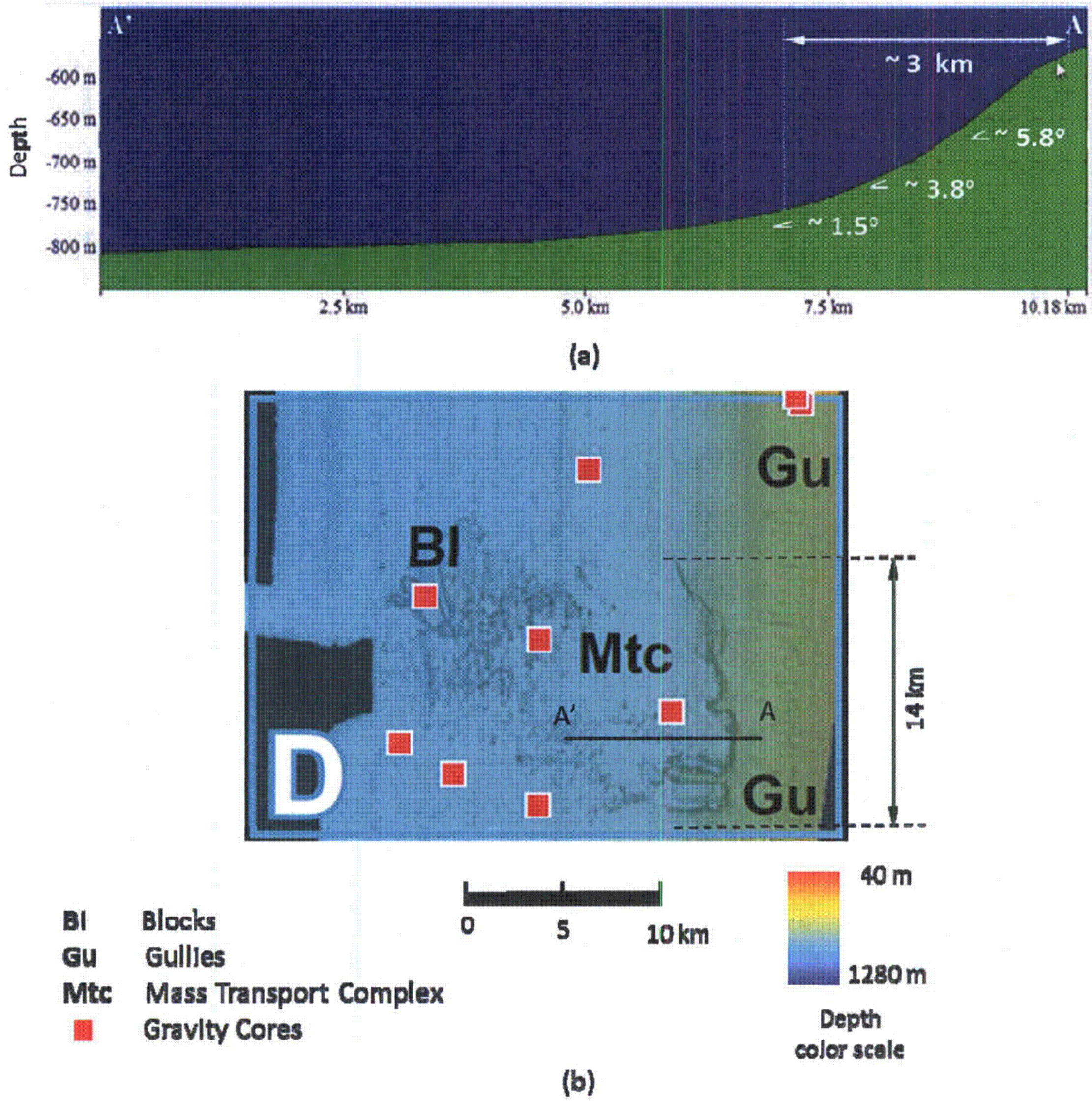

Note: The location of panel D is shown in Figure 34

Figure 36 Location of Postulated Slide Location Along the Great Bahama Bank and Location of Seismic Profiles

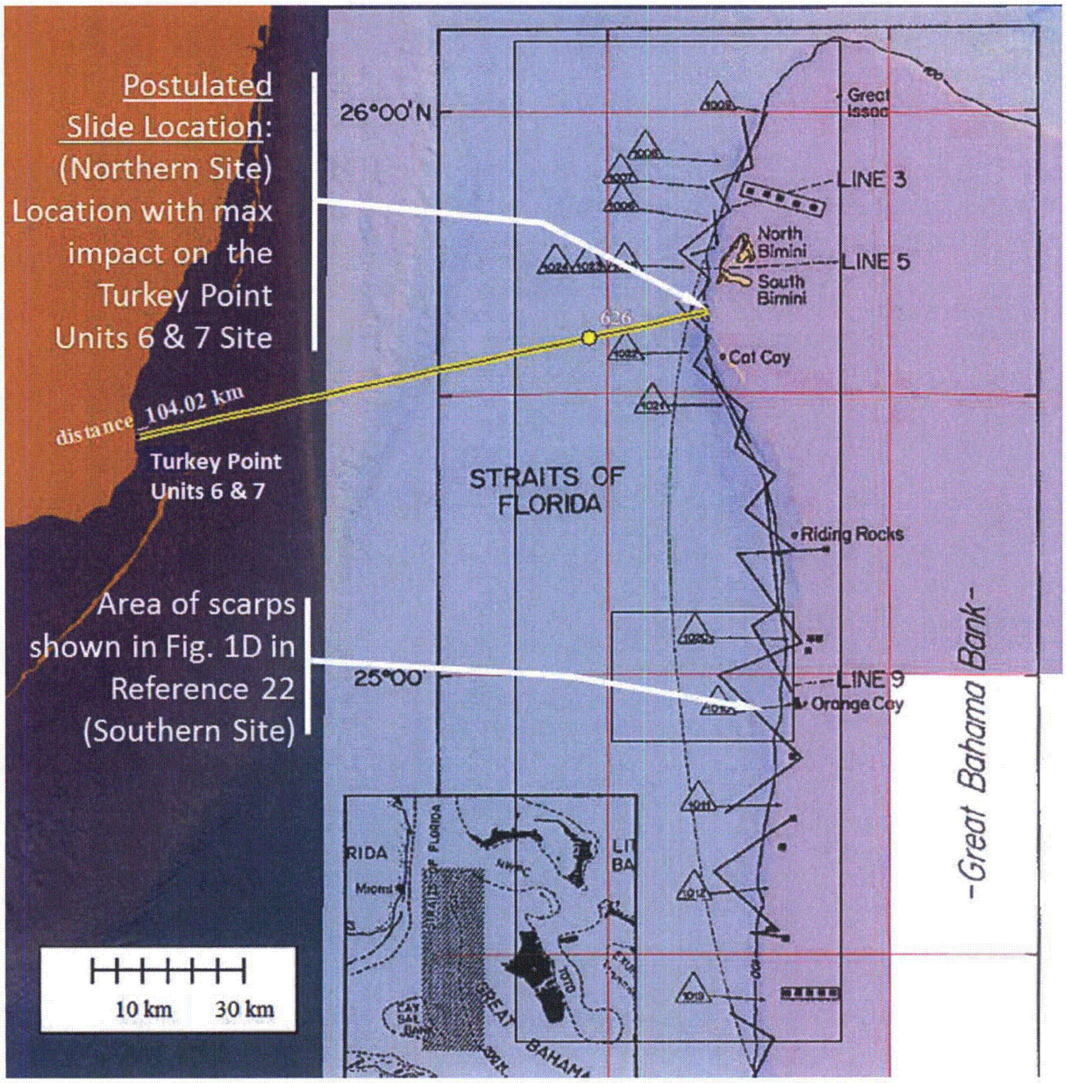

Source: Modified from Reference 24

Figure 37 Seismic Profile Line 5

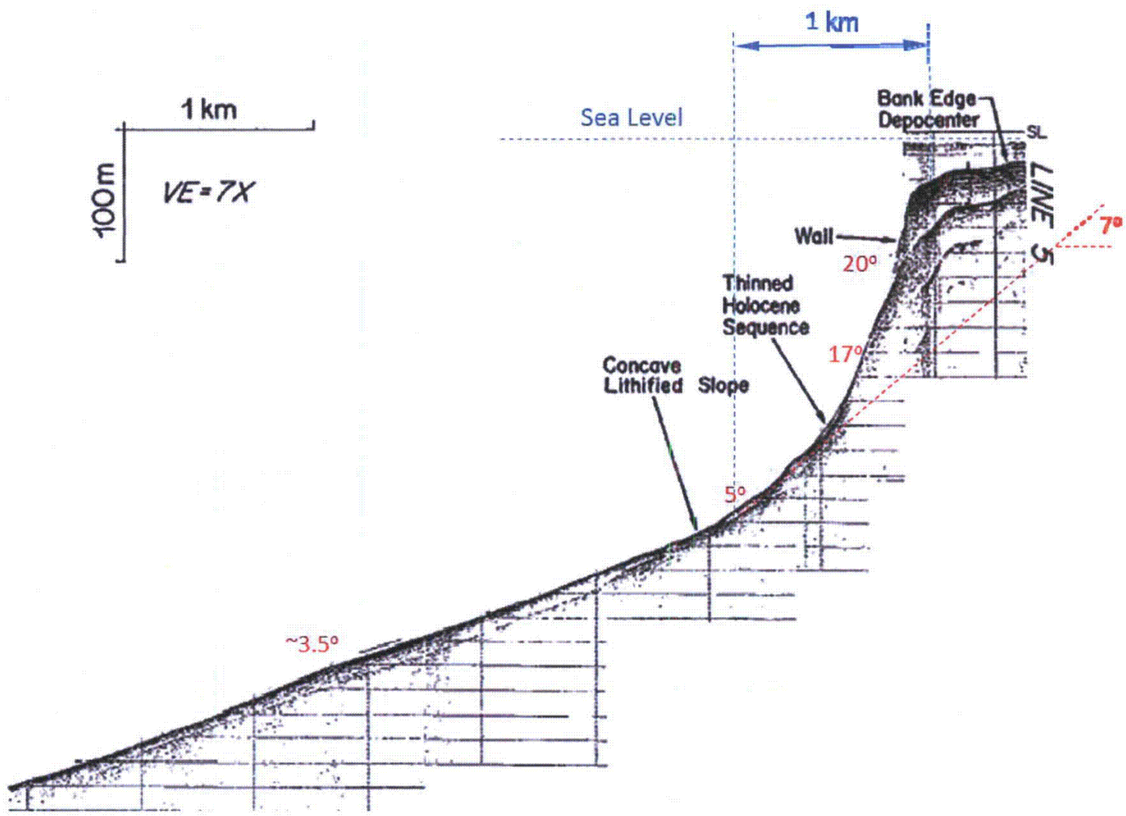

Notes: The location of this profile is shown in Figure 36.

VE represents Vertical Exaggeration.

Figure 38 Bathymetry in the Vicinity of the Postulated Slide Location

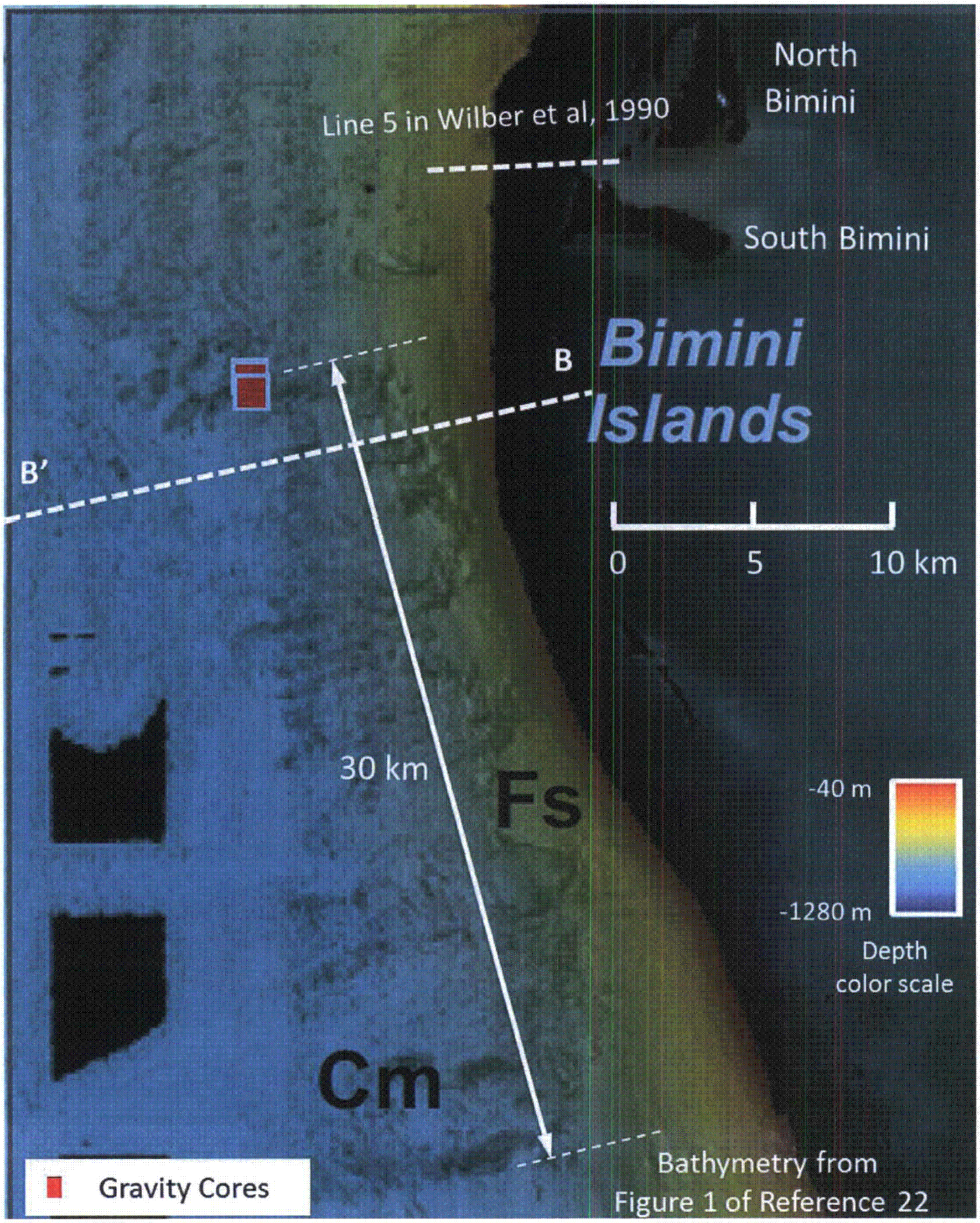

Source: Modified from Reference 22

Figure 39 Ocean Bottom Profile Along the Line B-B'

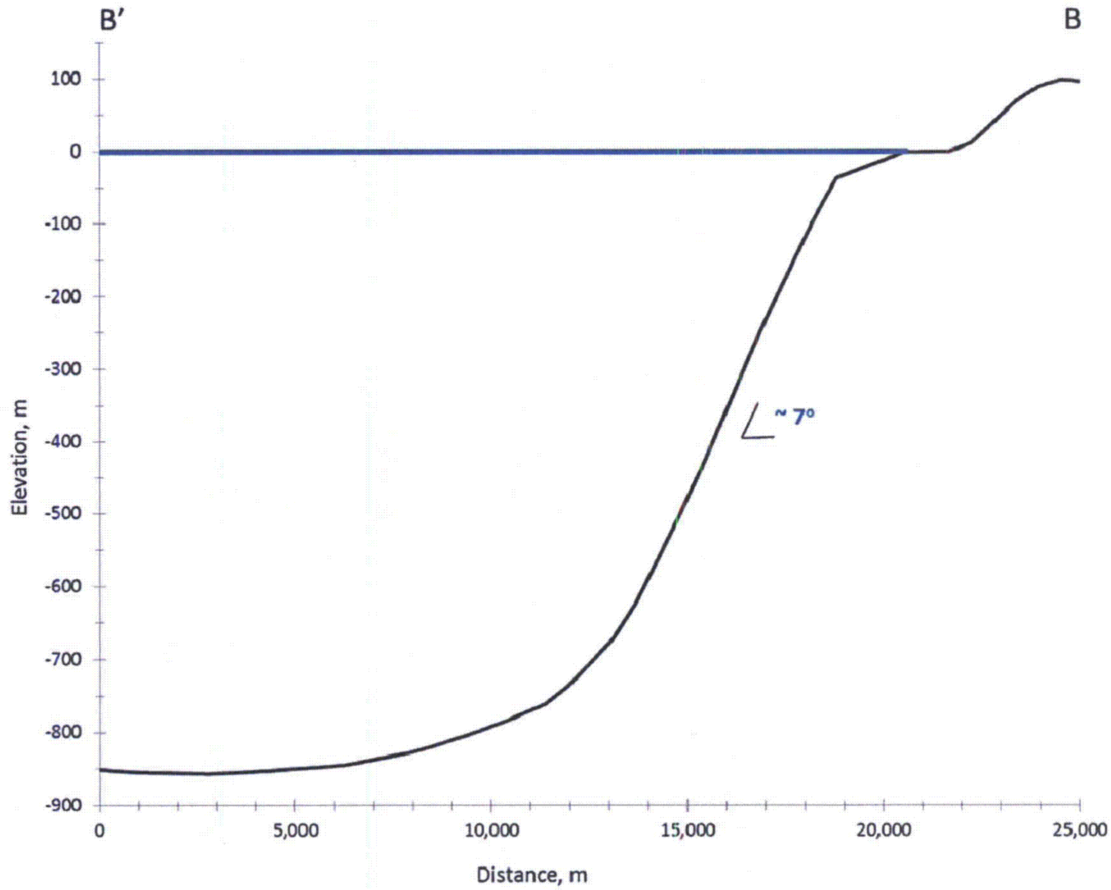

Note: The location of this profile is shown in Figure 38.

Figure 40 Grids Used in the Tsunami Simulations from Great Bahama Bank Slide

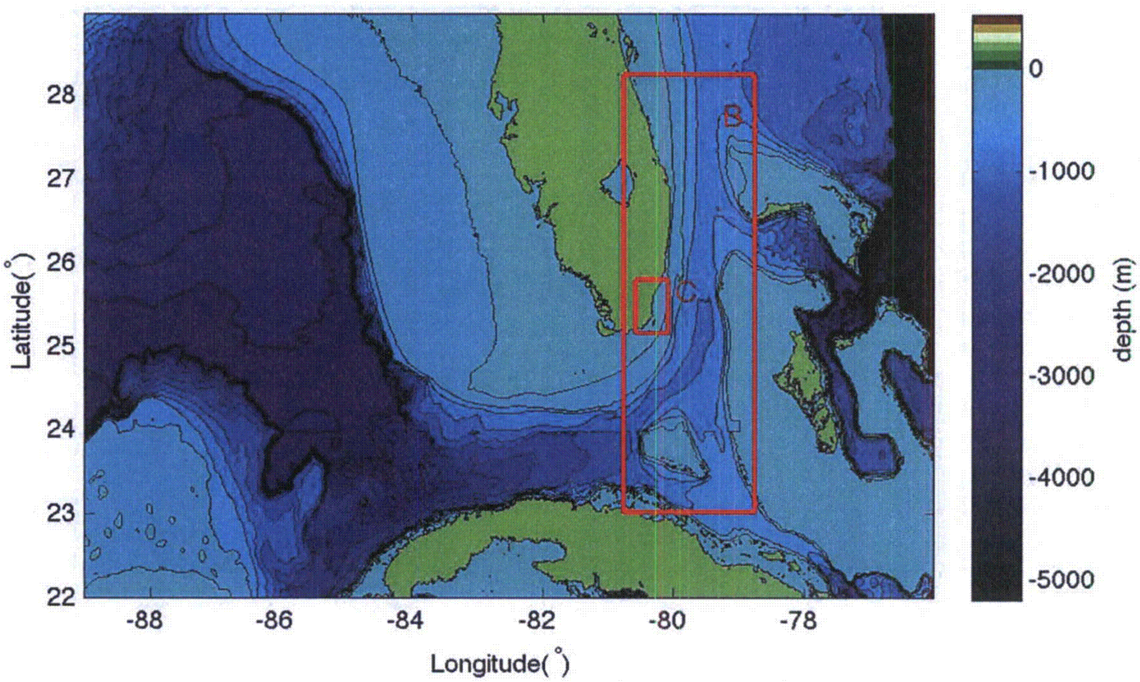

Figure 41 Location and Lateral Extent of the Postulated Slide Along the GBB

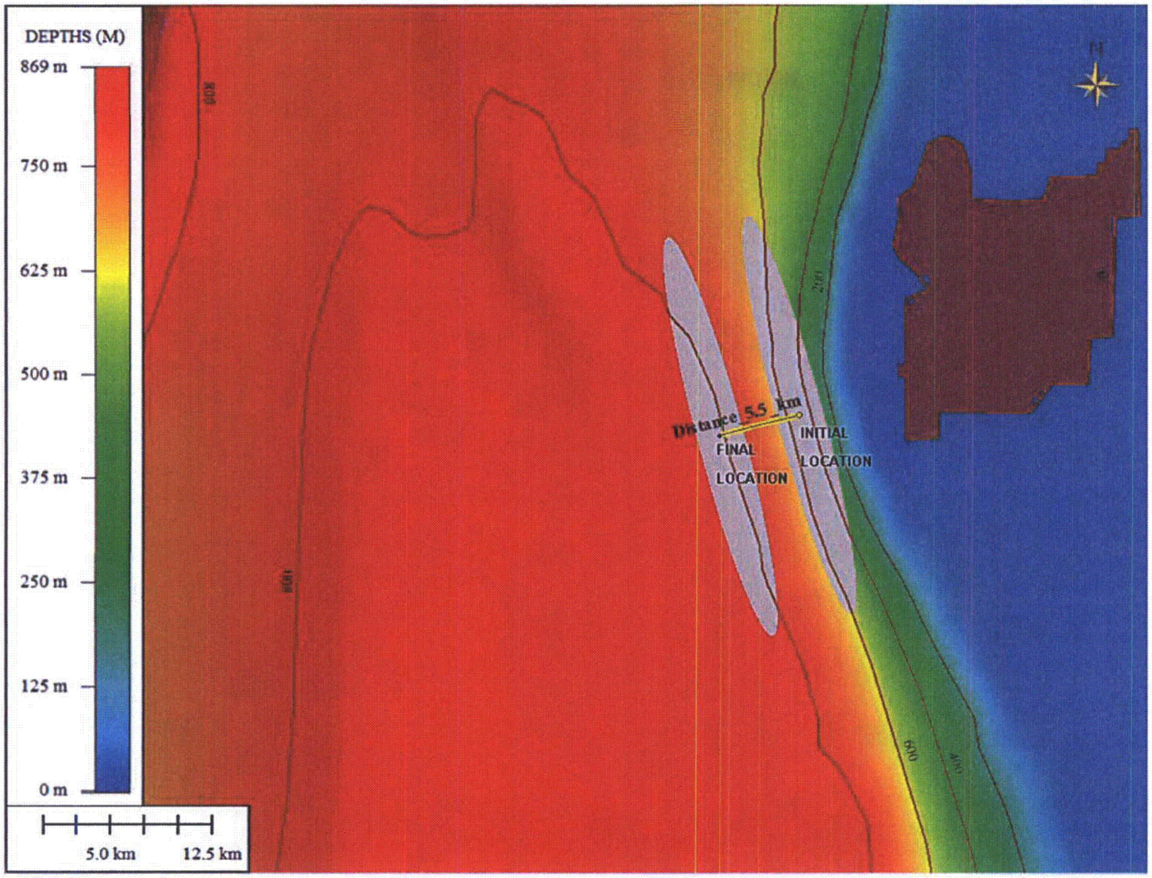

Note: Also shown are the approximate initial and final position of the slide at the end of the run-out distance for Case 1. Bathymetry contour elevations relative to MLW.

Figure 42 Initial Wave Generated by NHWAVE for Case 1 (Dynamic Source, 7 Degree Slope), at 110 Seconds after Initialization of the Slide

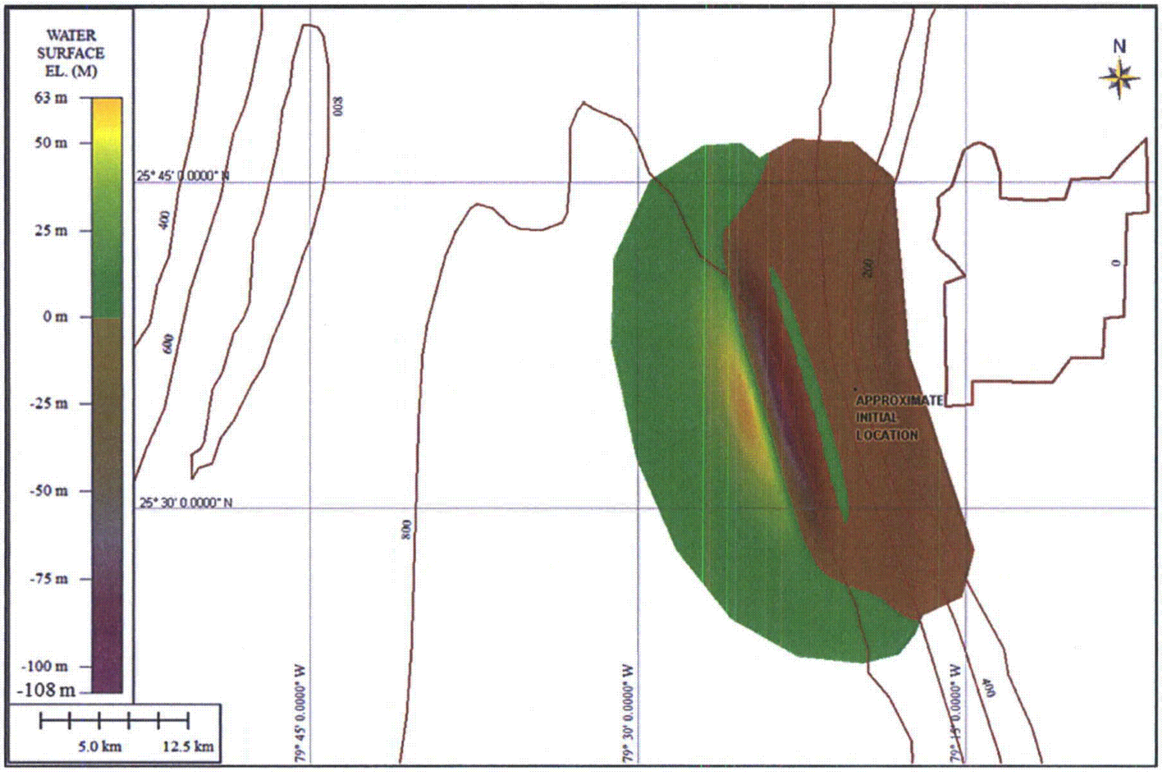

Figure 43 Case 1 (Dynamic Source, 7 Degree Slope): Water Surface Profiles in the Direction of the Slide Motion at Different Times After the Initiation of the Slide Obtained from NHWAVE

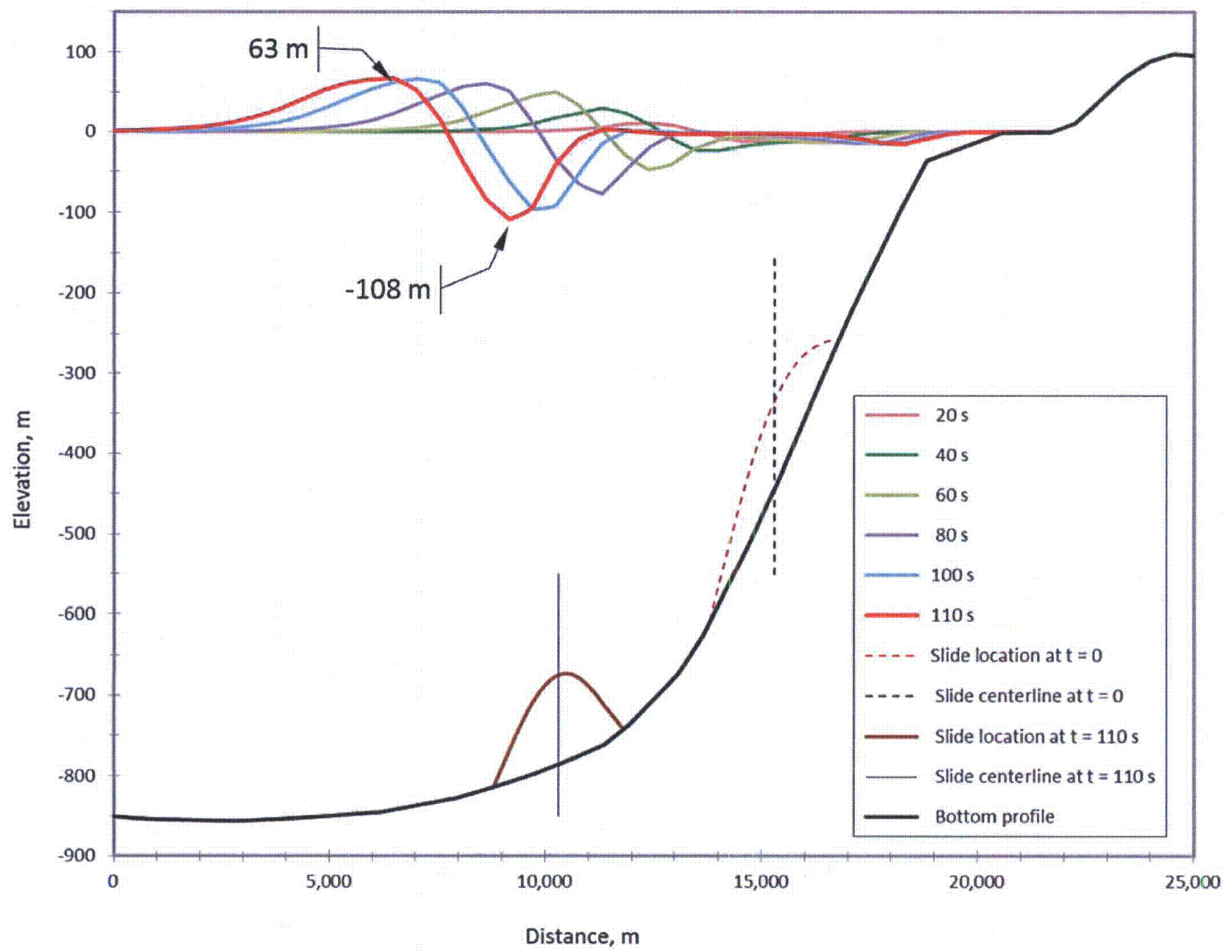

Note: The water surface profiles and cross section shown in this figure are along the minor axis of the ellipse shown in Figure 42, i.e., along the direction of the slide motion.

Figure 44 Case 1 (Dynamic Source, 7 Degree Slope): Simulated Propagation of the Tsunami Wave in Grid B at 2, 4, 6, and 14 Minutes After the Slope Failure in the GBB

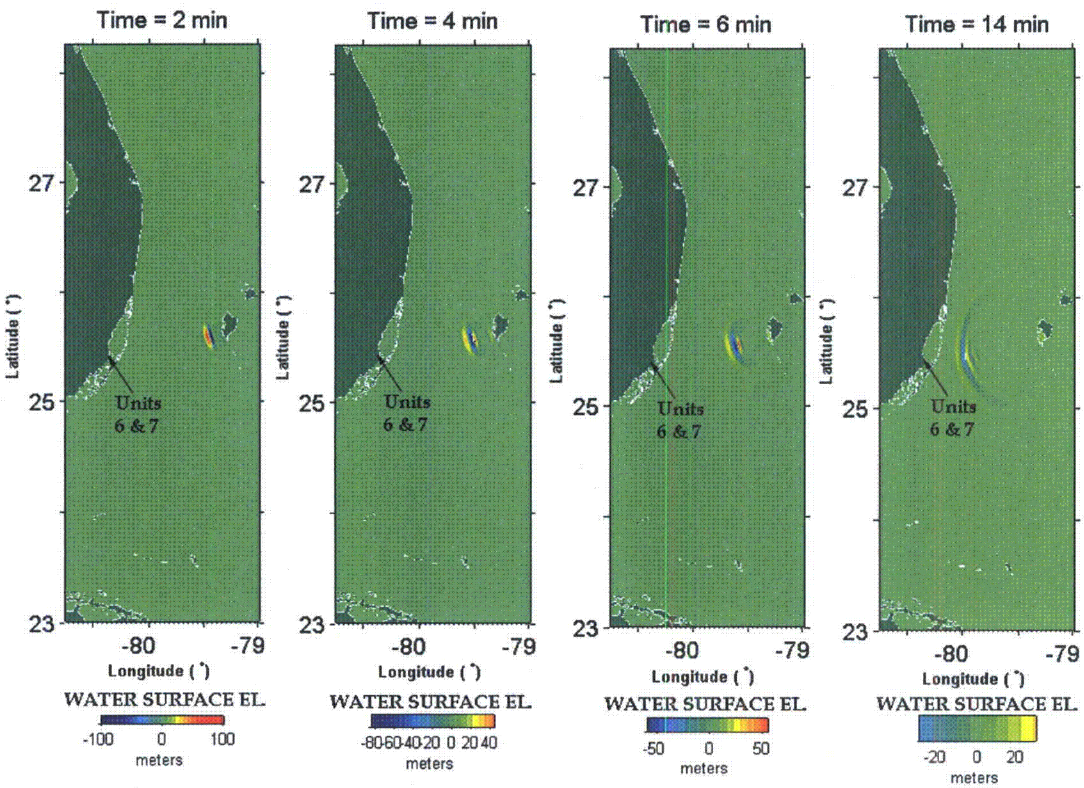

Notes:

1. The above time steps assume a hot-start initial condition.
2. The total time since initiation of the slide includes an additional 110 seconds (1.8 minutes).
3. Water surface elevations presented in the above figure are relative to the initial water surface level in FUNWAVE-TVD.
4. The initial water surface level in FUNWAVE-TVD is 1.68 meters MLW.

Figure 45 Case 1 (Dynamic Source, 7 Degree Slope): Simulated Maximum Wave Height in Grid B During the Propagation of the Tsunami Generated by the Slope Failure in the GBB

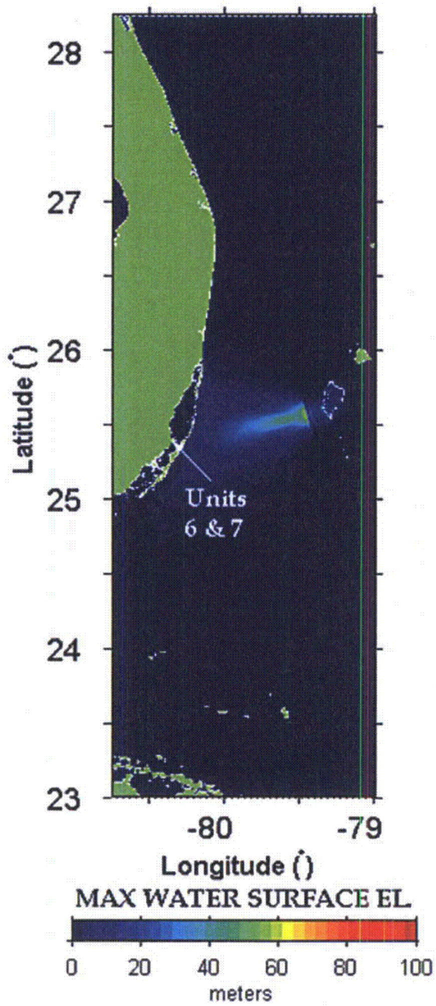

Notes:

1. Water surface elevations presented in the above figure are relative to the initial water surface level in FUNWAVE-TVD.
2. The initial water surface level in FUNWAVE-TVD is 1.68 meters MLW.